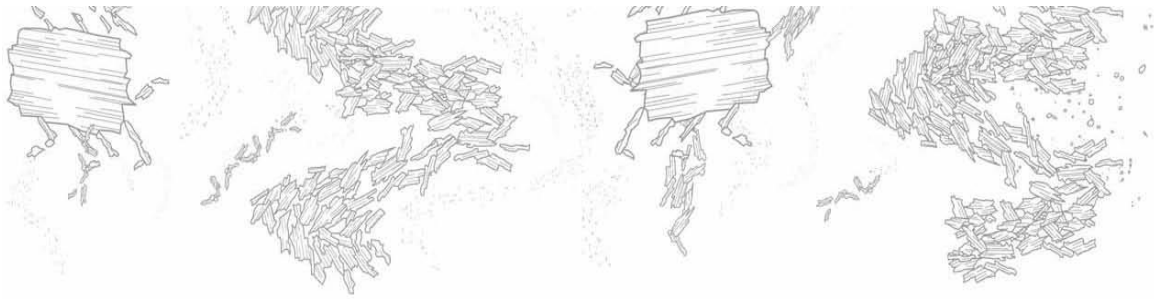

Structures and Textures of Metamorphic Rocks

Questions to be Considered in this Chapter:

1. What textures develop during the various types of metamorphism?
2. How do solid-state metamorphic textures differ from igneous (and sedimentary) textures, and how can we use those textures to interpret the style of and conditions accompanying metamorphism?
3. What processes occur within crystals and at grain boundaries during solid-state deformation, recrystallization, and/or reaction?
4. How can metamorphic textures be used to interpret the metamorphic, orogenic, and even pre-metamorphic history of rocks?
5. How can geochronology be linked more specifically to textural criteria to determine the age of specific (even multiple) events and the rates of metamorphic or tectonic processes?

I use the term **texture** to refer to small-scale features in a rock that are **penetrative**, meaning that the texture occurs in virtually all of the rock body at the microscopic scale. **Structures** are larger-scale features that occur on the hand sample, outcrop, or regional scale. Materials scientists, who typically work with metals or ceramics, use "texture" to refer strictly to preferred orientations. Several geologists (including the IUGS-SCMR) advocate conforming to the material science literature and using the term **micro-structure**, instead of texture, to describe any small-scale features of rocks. This relatively new usage, however, restricts the meaning of *texture*, as applied elsewhere in geologic literature, and it remains to see if it will be widely adopted. **Fabric** is also used by many geologists as a synonym for texture. I'm old fashioned, I suppose, and will stick with the definition of texture as first defined above.

This chapter concentrates on textures observable in thin section, although many may also be seen in hand specimen. Geology generally behaves like fractals because the structures seen on a regional scale (such as folding) are similar in style and orientation to those seen in the outcrop, hand specimen, and thin section. Petrographic data can thus be coordinated with petrology and structural geology as part of the ultimate goal of regional (and eventually global) synthesis of geologic history.

As in igneous rocks, the textures of metamorphic rocks reflect the combined processes of crystal nucleation, crystal growth, and diffusion of matter (Daniel and Spear, 1999). These processes, however, are generally more complex in solid-state metamorphic systems. For example, the growth of a new metamorphic mineral typically results from the reaction of other minerals that have become unstable. Some overstepping of the actual *P-T* boundary conditions is usually necessary before any reaction is really effective, particularly under lower temperature metamorphic conditions. Except for some cases of polymorphic transformations, metamorphic mineral growth generally involves:

1. Detachment of ions from the surface of reacting minerals (presumably dissolving into a small amount of intergranular fluid in most situations)
2. Nucleation of the new mineral(s)

From Chapter 23 of *Principles of Igneous and Metamorphic Petrology*, Second Edition, John D. Winter.

3. Diffusion of material to the sites of new mineral growth
4. Growth of the new mineral(s), incorporating components carried to the surface and transportation of excess waste constituents away

The step that is slowest under any set of conditions is the *rate-determining* step for the process.

The combined effects of deformation and recovery–recrystallization, as well as variations in the timing of deformation versus crystallization, make for more textural variability in metamorphic rocks than is common in igneous ones. The majority of these effects leave clear textural imprints, but the interaction of several processes and the repetition of some make it more challenging to interpret metamorphic histories on the basis of textural criteria.

In most cases, the principles behind textural interpretation are clear and relatively simple, but the application of the principles may at times be ambiguous. In this chapter, we shall attempt to review the principles involved so that we can interpret the processes responsible for the development of a metamorphic rock by careful observation of the products.

First, let's define a few basic textural terms that will make the ensuing discussion easier. The suffix **-blast** or **-blastic** indicates that a feature is of metamorphic origin. Thus **porphyroblastic** means a porphyritic-like texture (large grains in a finer matrix) that is of metamorphic origin. Regrettably, the *prefix* **blasto-** (meaning that a feature is *not* of metamorphic origin but is inherited from the parent rock) is too easily confused with the *suffix* form meaning just the opposite. For example, *blastoporphyritic* indicates an igneous porphyritic texture that survived metamorphism to the extent that it can still be recognized. The similarity between *blastoporphyritic* and *porphyroblastic*, and numerous other such pairs, is unfortunate. The term **relict**, like the prefix blasto-, indicates that a feature is inherited from the protolith. We can thus speak of relict bedding in metasediments, or relict porphyritic texture, or even of individual relict minerals. Because of the blasted confusion associated with the prefix and suffix forms of *blast*, I prefer to use the term *relict* rather than the prefix *blasto-*.

Perfectly straightforward terms such as euhedral, subhedral, and anhedral (indicating progressively less-well-shaped crystals) have been replaced in some of the metamorphic literature with **idioblastic**, **hybidioblastic**, and **xenoblastic**, respectively. The terms stem from somewhat dated general ones (idiomorphic, hypidiomorphic, etc.), but I doubt that a clear metamorphic distinction justifies the inflation of our lexicon in this case, and I prefer the simple universal terms listed first. The metamorphic terms are well established, however, and useful in some contexts.

The IUGS-SCMR recommended use of *phaneritic* and *aphanitic* as grain size terms, following the usage advocated for igneous rocks (Fettes and Desmons, 2007). The IUGS-SCMR recommended that other grain size terms not be associated with any absolute values because there are no universal standards. For those stubbornly requiring absolute values, however, the IUGS-SCMR suggested the following scheme (numeric values in parentheses represent the limiting diameters): ultra-fine grained (0.01 mm), very fine grained (0.1 mm), fine grained (1 mm), medium grained (4 mm), coarse grained (16 mm), and very coarse grained. That these limits do not correlate to those recommended for igneous rocks seems to strengthen the IUGS-SCMR's point.

In what follows, I shall attempt to summarize the principal mechanisms of solid-state deformation and recrystallization, followed by a review of the textures characteristic of the three principal types of metamorphism: contact, regional/orogenic, and fault zone. For a more detailed analysis, see the excellent summaries of metamorphic textures and deformation mechanisms by Passchier and Trouw (2005) and Vernon (2004).

1 THE PROCESSES OF DEFORMATION, RECOVERY, AND RECRYSTALLIZATION

Deformation of crystalline solids involves a number of processes, several of which may work in unison. The dominant processes at any particular time depend on both intrinsic rock factors (mineralogy; grain size and orientation; and the presence, composition, and mobility of intergranular fluids) and externally imposed factors (temperature, pressure, deviatoric stress, fluid pressure, and strain rate). The principal deformation mechanisms are listed below in the general order of increasing temperature and/or decreasing strain-rate, following the approach of Passchier and Trouw (2005).

1. Cataclastic flow is the mechanical fragmentation of a rock and the sliding and rotation of the fragments. These brittle processes include frictional grain-boundary sliding and fracture (Vernon, 2004). The products are fault gouge, breccia, or cataclasite.

2. Solution transfer (Figure 1), also called **pressure solution**, requires intergranular fluid to be effective. Grain contacts at a high angle to σ_1 (the shortening direction) become highly strained and have higher energy. The material at these contacts dissolves more readily as a result of the higher energy and produces higher concentrations of dissolved species at these locations. This, in turn, sets up an activity gradient so that dissolved species migrate from high activity to low activity places (which are also low-strain places) where the material precipitates.

3. Intracrystalline deformation of a plastic type involves no loss of cohesion in the rock. Several processes may be involved, often simultaneously. Simple torquing and bending of bonds in a crystal is elastic and quickly recoverable. *Permanent* deformation requires more significant changes in the position of atoms/ions, typically involving the breaking of chemical bonds. In intracrystalline deformation, this happens most easily by movement of lattice **defects**. (Defects are described in most mineralogy texts and can be imaged and studied by electron microscopy techniques.) **Point defects** include *vacancy* and *interstitial* types, and **line defects** include *edge* and *screw dislocations*. There is also a variety of combined defects.

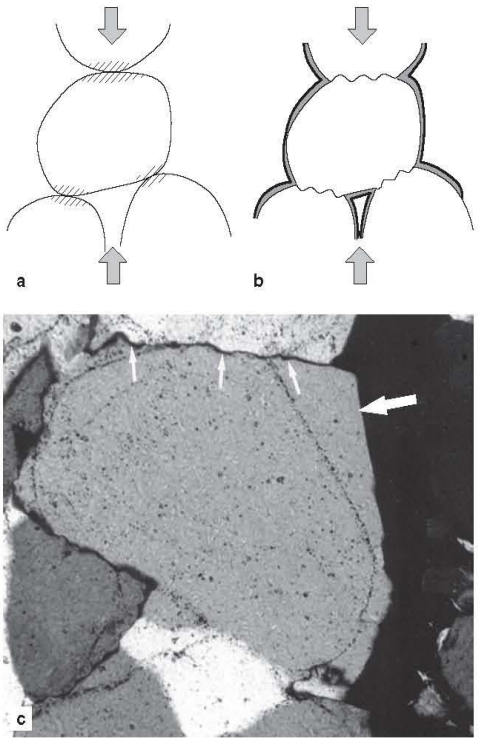

FIGURE 1 Pressure solution in grains affected by a vertical maximum stress and surrounded by a pore fluid. **(a)** Highest strain in areas near grain contacts (hatch pattern). **(b)** High-strain areas dissolve and material precipitates in adjacent low-strain areas (shaded). The process is accompanied by vertical shortening. **(c)** Pressure solution of a quartz crystal in a deformed quartzite (σ_1 is vertical). Pressure solution results in a serrated solution surface in high-strain areas (small arrows) and precipitation in low-strain areas (large arrow). ~0.5 mm across. The faint line within the grain is a hematite stain along the original clast surface. After Hibbard (1995).

Figure 2 illustrates lattice deformation via a process of vacancy migration to accommodate stress by shortening (flattening). Figure 3 shows accommodation of shear by edge-dislocation migration. Defect migration in either case is crystallographically controlled and can happen only along certain **slip directions** in certain **slip planes**; the combination is called a **slip system**. Both processes in the two figures allow deformation to occur by displacing only a tiny part of a crystal at a time, thus permitting strain to occur with much less deviatoric stress than if the whole lattice had to yield along a fracture at once. Defects, in other words, weaken rocks. Point defect migration also enhances *diffusion* through a lattice because the motion of a vacancy in one direction is equivalent to migration of matter in the opposite direction.

Dislocation glide involves the migration of dislocations along a slip system (as in Figure 3). Most plastically or ductilely deformable crystals (quartz, carbonates, ice) have several potential slip systems with different orientations, which enhances their capacity to accommodate stress. When glide along different active slip systems intersects,

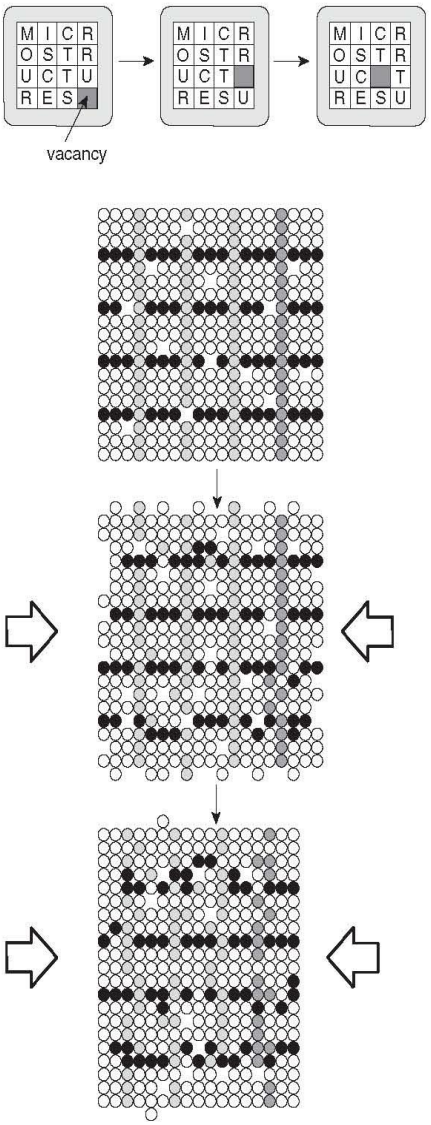

FIGURE 2 **(a)** Migration of a vacancy in a familiar game. **(b)** Plastic horizontal shortening of a crystal by vacancy migration. From Passchier and Trouw (2005). Copyright © with permission from Springer-Verlag.

migrating dislocations can interfere, forming dislocation "tangles," inhibiting further motion on all slip systems. A greater degree of differential stress is then required to overcome the tangle and permit slip. Because more stress is required for deformation, material with numerous tangles is effectively stronger. This is called **strain hardening**. Obstructions can be overcome by **dislocation creep**, in which vacancies migrate to the dislocations and allow them to "climb" over a blocked site.

As dislocations form and migrate, portions of a crystal's lattice become reoriented. An easily observed result of this is **undulose extinction** (Figure 4), because the extinction position of a mineral under the polarizing

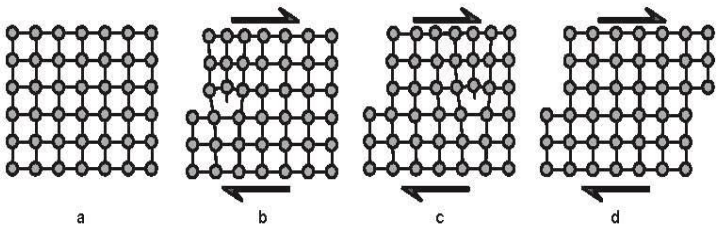

FIGURE 3 Plastic deformation of a crystal lattice (experiencing dextral shear) by the migration of an edge dislocation (as viewed down the axis of the dislocation).

microscope is dependent upon its crystallographic orientation. **Deformation twinning** can also accommodate a limited amount of strain in specific crystallographic directions. It is common in calcite and plagioclase. Because some slip and twin directions are more effective than others, deformation can cause crystals to reorient themselves to more easily accommodate an imposed stress, resulting in **lattice preferred orientation** (**LPO**) of many of the crystals in a deformed rock.

4. Recovery. Permanent strain in crystals depends largely on defects. The magnitude of the strain, unless somehow relieved, is proportional to the density of defects in a crystal. Stored strain energy decreases the stability of a mineral and can be lowered by migration of defects in the following ways:

- Migration of vacancies to dislocation tangles straightens out blocked and tangled areas.
- Dislocations that are bent can straighten out by their migration.
- Dislocations can migrate and arrange themselves into networks.
- Dislocations of opposite sense that migrate and meet will annihilate one another.

These mechanisms constitute *recovery*. During deformation, the formation and disorderly migration of defects competes with the recovery processes, so that the stored strain energy reaches some constant value dependent on strain rate, temperature, etc. When deformation wanes, recovery predominates (if the temperature is sufficiently high), and the dislocation density and strain energy are greatly reduced.

Figure 5 illustrates the migration of scattered dislocations to planar arrays, or "dislocation walls." This takes a strained crystal and creates two distinct unstrained **subgrains**. Subgrains are portions of a grain in which the lattices differ by a small angle (the misorientation angle is exaggerated in Figure 5b). *Separate* grains differ in that they have high-angle misorientations. Figure 4b shows elongate subgrains in a single larger quartz grain. Note that the number of dislocations in Figure 5 may be the same (although some annihilation of dislocations of opposite sense may reduce it), but the *density* of subgrain dislocations (if you consider the subgrains separately) is much smaller, as is the total lattice strain. Note that subgrains also produce undulose extinction, but more abruptly at the boundaries of the extinction domains, which are much sharper and correspond to "dislocation walls."

5. Recrystallization is another way to reduce stored lattice strain energy. Recrystallization involves the movement of grain boundaries or the development of new boundaries, both of which produce a different configuration of *grains* (with high-angle orientation differences from neighbors), not *subgrains*.

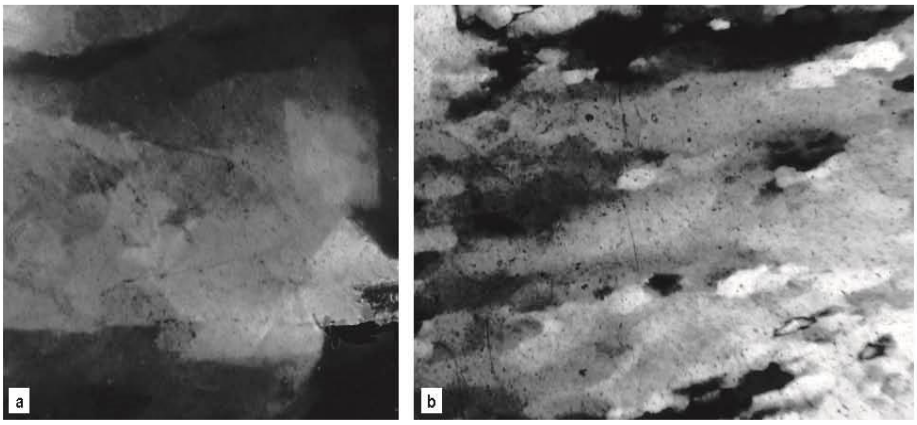

FIGURE 4 (a) Undulose extinction in quartz. 0.2 mm across. (b) Elongate subgrains in deformed quartz, also undulose. 0.7 mm across.

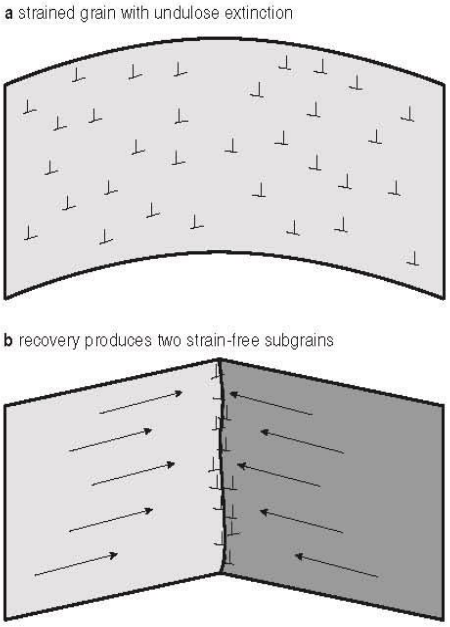

FIGURE 5 Illustration of a recovery process in which dislocations migrate to form a subgrain boundary.

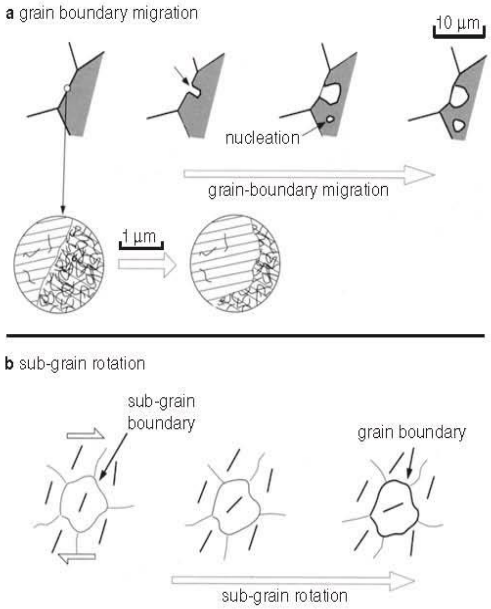

FIGURE 6 Recrystallization by (a) grain-boundary migration (including nucleation) and (b) subgrain rotation. From Passchier and Trouw (2005). Copyright © with permission from Springer-Verlag.

Recrystallization occurs by grain boundary migration or subgrain rotation (Figure 6). In **grain boundary migration** (Figures 6a and 7a), the atoms in a grain with higher strain energy migrate by diffusion and add to a neighboring grain with lower strain energy (also called **bulging**). Less commonly, an isolated new grain may nucleate in a highly strained area of a deformed grain. **Subgrain rotation** (Figure 6b) occurs when dislocations are free to creep from the lattice plane of one subgrain to that of another and add (almost continuously) to a neighboring subgrain. The added dislocations cause the receiving subgrain lattice to rotate until it is sufficiently different from its neighbors to qualify as a separate

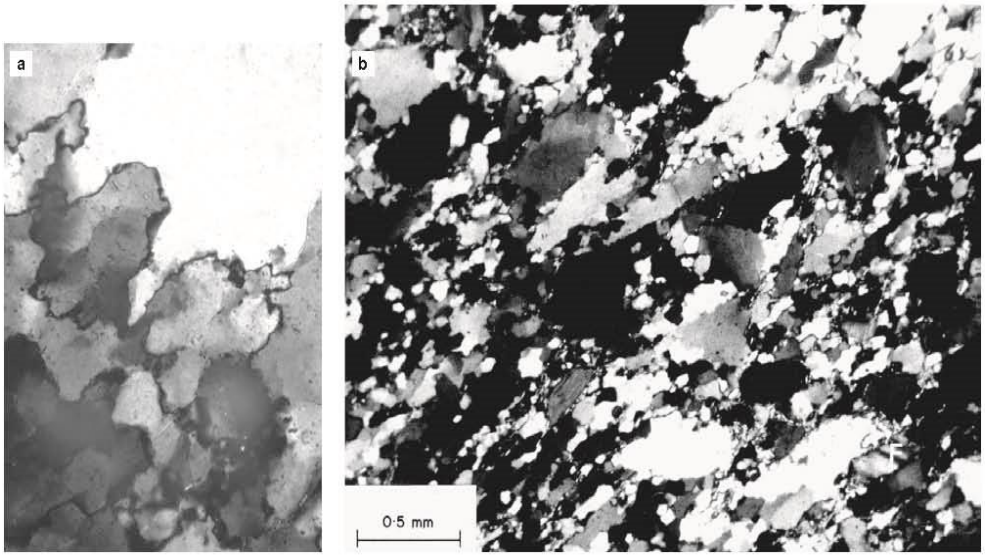

FIGURE 7 (a) Recrystallized quartz with irregular (sutured) boundaries, formed by grain boundary migration. Width 0.2 mm. (b) Deformed polycrystalline quartz with a foliation attributed to rotation of grains plus intracrystalline slip. Small grains are probably formed by subgrain rotation recrystallization. From Borradaile et al. (1982). Copyright © with permission from Springer-Verlag.

grain. Figure 7b shows irregular quartz grains with both low-angle subgrains and high-angle grains, the latter probably created by subgrain rotation. These two forms of recrystallization may occur during deformation as well as after deformation ceases.

At higher temperatures, crystals can deform solely by the migration of vacancies through the lattice (Figure 2). This process is called **solid-state diffusion creep**. **Crystalplastic deformation** is a loose term used to describe deformation by a combination of dislocation and diffusion creep. In fine-grained aggregates, crystals may also slide past one another by **grain boundary sliding**. Voids between sliding crystals are prevented by solid-state diffusion creep or solution-precipitation involving a fluid. At such high temperatures the rocks are weak, and deformation may be rapid.

A final recrystallization process is **grain boundary area reduction**. Grain boundaries are surfaces where lattices end, and bonds are unsatisfied. The high energy of these boundaries constitutes a smaller percentage of the volume of a rock when crystals become coarser (a smaller surface-area-to-volume ratio) and/or when boundaries become straighter. Both of these processes constitute grain boundary area reduction and reduce the overall energy of the rock. Ostwald ripening is a form of grain boundary area reduction in which grain boundaries migrate in the direction of curvature, thereby eliminating smaller grains and enlarging others as grain boundaries are straightened. Reduction in the free energy of a rock system by grain boundary area reduction is generally much less than by other recovery or recrystallization processes. It cannot keep pace with deformation, and its effects are much more obvious and dominant after deformation ceases, especially at high temperatures.

Recovery and recrystallization are temperature-dependent processes. They are slow at low temperatures but increase quickly at a threshold temperature *that depends on the minerals involved*. Some minerals may thus behave in a brittle fashion, whereas other coexisting minerals are more plastic. For example, in a deforming granite at shallow depths quartz is usually stronger than feldspar, but both are brittle and deform by fracture. At slightly greater depths where temperatures reach 200 to 300°C, quartz becomes ductile and loses strength, whereas feldspars remain brittle. The resistant feldspars typically form augen in the more ductile matrix of quartz and micas (Figure 18). At higher temperatures both quartz and feldspar behave in a more ductile fashion.

There is an important interrelationship between deformation and recovery–recrystallization. Deformation creates strain in grains (raising lattice energy), which, in turn, drives the processes of recovery and recrystallization (which lower lattice energy). Recovery has a lower threshold energy than recrystallization, so it occurs more readily. Recovery typically produces irregular and interlocking grain boundaries (called **serrated** or **sutured** grain boundaries, shown in Figures 7a and 15b), as highly strained material at grain boundaries is incorporated onto either of the adjacent larger crystals by grain boundary migration and subgrain rotation. More advanced recrystallization, on the other hand, tends to eliminate the suturing by grain boundary area reduction. In some cases, the processes of deformation and recovery–recrystallization act in unison. The combined process is called **dynamic recrystallization**, which usually produces elongated grains and well-developed schistosity. Under low-temperature and dry conditions, recrystallization may be impeded, but at higher temperatures (especially with aqueous fluids present), **static recrystallization** or **annealing** (consisting of recovery, recrystallization, and grain boundary area reduction) may be common. Recovery and recrystallization may completely overcome lattice strain if temperature remains high following deformation in orogenic belts, and minerals aligned by dynamic recrystallization into a well-developed schistosity may retain little or no intracrystalline strain. Recrystallized textures also predominate in contact metamorphic aureoles where the temperature was high and deviatoric stress was low.

Deformation may also provide the extra energy required to overcome kinetic barriers to reactions. Figure 8 shows an outcrop in southwestern Norway where crustal rocks were subducted deeply during the Caledonian orogeny. Reaction from unstable (plagioclase–hornblende) amphibolites to stable (clinopyroxene–garnet) eclogites at the pressures involved proceeded only where the strain was high within a shear zone. Without the extra instability of strain-induced lattice energy (plus perhaps introduction of fluids along the shear zone, which may also enhance reactivity), the amphibolites outside the shear zone resisted reacting. Baxter and DePaolo (2004) noted that reaction rates in natural settings are generally orders of magnitude faster than in the lab and just slower than associated strain rates (Section 7). They argued that strain-induced grain boundary migration and diffusion creep expose grain interiors to the intergranular transport medium, thereby enhancing diffusion of material to the sites of new mineral growth during reactions. If so, strain

FIGURE 8 Gneissic anorthositic–amphibolite (light color on right) reacts to become eclogite (darker on left) as left-lateral shear transposes the gneissosity and facilitates the amphibolite-to-eclogite reaction. Bergen area, Norway. Two-foot scale. Courtesy of David Bridgwater.

may commonly control reaction progress and explain why reaction rates are usually slightly slower than strain rates and faster in nature than in static lab experiments. Although strain may permit reactions to proceed toward equilibrium, it cannot change the nature of the equilibrium mineralogy, as was once proposed for "stress minerals" that were mistakenly believed to form only under conditions of deviatoric stress.

2 TEXTURES OF CONTACT METAMORPHISM

Contact metamorphism occurs in aureoles around intrusive bodies and is a response of cooler country rocks to the thermal ± metasomatic effects of the intrusion. The textures of contact metamorphism are typically developed at low pressures and thus under conditions of low deviatoric stress. The thermal maximum in a contact aureole should also occur much later than any stress imparted by forceful intrusion. Crystallization (including recrystallization) may therefore occur in a near-static environment, and contact metamorphism is typically characterized by a lack of significant preferred mineral orientation. Many minerals are equidimensional, rather than elongated, and the elongated minerals that do form are orientated randomly. Relict textures are also common in contact metamorphic rocks because there is little accompanying shear to destroy them.

Static recrystallization occurs after deformation ceases at elevated temperatures or when a thermal disturbance occurs in a low-stress environment. As described above, the process acts to reduce both lattice strain energy and overall surface energy. The textures that result typically depend on the minerals involved. In "structurally anisotropic" minerals, the surface energy of a grain boundary depends strongly on the lattice orientation of the boundary in question, whereas in "structurally isotropic" minerals the grain boundary energy is about the same for any surface. If the orientation dependence is low (as in quartz or calcite), no particular faces are preferentially developed. Thus in *monomineralic* aggregates of structurally isotropic minerals (quartzites or marbles), grain boundary area reduction leads to an equilibrium texture in which grains meet along straight boundaries (resulting in low surface area for each grain). The texture is called **granoblastic polygonal** (or **polygonal mosaic**), and grains appear in two-dimensional thin sections as equidimensional polygons with grain boundaries that meet in triple junctions with approximately 120° between them (Figure 9a). The size of the polygonal grains depends mainly on temperature and the presence of fluids (higher temperatures and aqueous fluids promote larger crystals).

Structurally anisotropic minerals, such as micas and amphiboles, have some crystallographic surfaces with much lower energy than others. This affects the shape of the grains, and thus the equilibrium recrystallization texture. High surface energy boundaries grow faster, so that low-energy

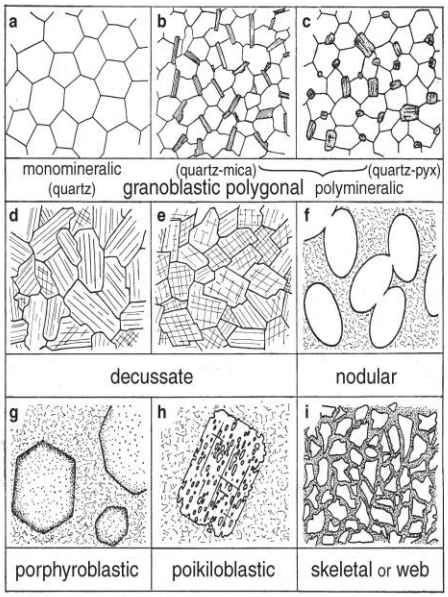

FIGURE 9 Typical textures of contact metamorphism. From Spry (1969).

surfaces become larger. To understand this, imagine a cube on a table. If the four vertical faces are of higher energy (less stable) and grow more quickly than the top and bottom faces, the cube will expand laterally faster than it does vertically, and it gradually becomes more plate-like. Low-energy surfaces in such minerals (e.g., the top and bottom of the plate) predominate in the final static recrystallization texture, even in monomineralic rocks, so that simple regular polygons are no longer abundant. The result is called **decussate** texture (Figures 9d and e).

In *polymineralic* rocks, the grain boundary energy also depends on whether the boundary is between like minerals or unlike minerals. In general, same-mineral (A-A) grain boundaries have higher energy than different-mineral (A-B) boundaries, so that the final static equilibrium texture will tend to minimize the total area of A-A boundaries and increase the area of A-B boundaries (thereby resulting in lower total energy). This brings us back to the concept of **dihedral angles**. In Figure 10, if the dihedral angle, θ, becomes smaller, the total area of A-B grain boundaries increases with respect to A-A boundaries. Polymineralic rocks thus develop a modified type of granoblastic texture in which 120° angles occur only at A-A-A or B-B-B triple junctions, and the other junctions depend on the relative grain-boundary energies of the different minerals involved (Figure 10c). Figure 9b and c also illustrate modified polygonal textures of polymineralic aggregates of quartz–mica and quartz–pyroxene, respectively.

In highly structurally anisotropic minerals in which the energy of one face is unusually low, such as {001} in mica, that face will predominate and will not be altered

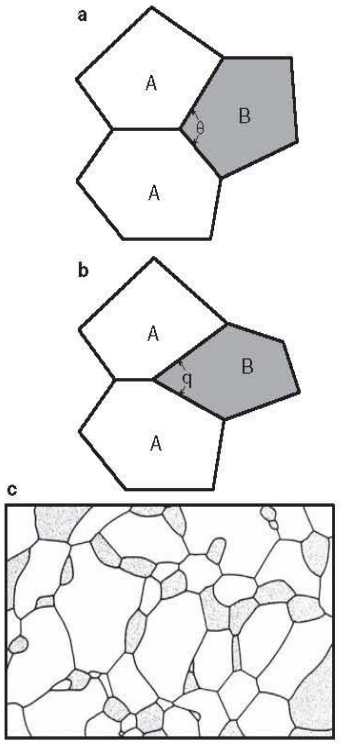

FIGURE 10 (a) Dihedral angle between two mineral types. When the A-A grain boundary energy is greater than for A-B, the angle θ will decrease (b) so as to increase the relative area of A-B boundaries. (c) Sketch of a plagioclase (light)-clinopyroxene (dark) hornfels showing lower dihedral angles in clinopyroxene at most cpx-plag-plag boundaries. (c) from Vernon (1976).

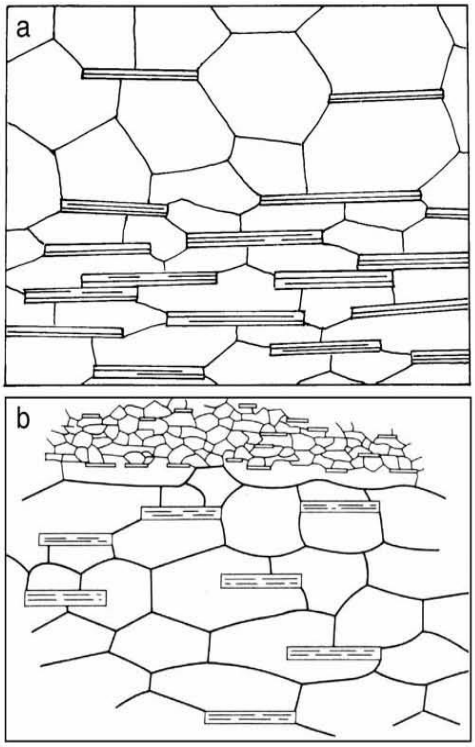

FIGURE 11 Drawings of quartz–mica schists. (a) Closer spacing of micas in the lower half causes quartz grains to passively elongate in order for quartz–quartz boundaries to meet mica (001) faces at 90°. From Shelley (1993). (b) Layered rock in which the growth of quartz has been retarded by grain boundary "pinning" by finer micas in the upper layer. From Vernon (1976).

much by the interfaces of more isotropic minerals such as quartz (Figure 9b). As a result, quartz–quartz interfaces usually intersect {001} faces of mica at right angles or join to the edges of mica flakes (Figure 11). In situations where micas are foliated and closely spaced, this tendency for right-angle intersections may cause the quartz grains to be elongate (Figure 11a, lower half), contrary to their usual tendency. This dimensional elongation is not caused by deformation of the quartz crystals but is an artifact of quartz conforming to the mica foliation.

Another common feature of polymineralic rocks is that the occurrence of a minor phase, such as graphite, may retard grain boundary migration of a more abundant phase and "pin" (or anchor) the boundaries, resulting in a finer grain size than might otherwise have occurred (Figure 11b).

Although not restricted to contact metamorphic rocks, **porphyroblasts** (Figure 9g) are very common. In examples of contact metamorphism, the rocks are typically characterized by large porphyroblasts of biotite, andalusite, or cordierite.

Poikiloblasts are porphyroblasts that incorporate numerous inclusions (equivalent to poikilitic texture in igneous rocks). This texture is common in garnet, staurolite, cordierite, and hornblende. Poikiloblastic texture (Figure 9h) is a high-energy texture because it represents a high surface area situation. It probably occurs as a result of poor nucleation and rapid porphyroblast growth, which envelops neighboring grains. In some cases, a high grain boundary energy between inclusion minerals may be reduced by the formation of a layer of another (poikiloblast) mineral between them. The surface energy of an included mineral is also lowered by rounding the edges, which is common among poikiloblast inclusions. Some inclusions may be inert phases that were passed up by the advancing front of the poikiloblast growth. Most, however, are believed to be a co-product of the poikiloblast-forming reaction, or a reactant that wasn't completely consumed. Poikiloblast thus typically grow at the same time as their inclusions, although at a faster rate (Vernon, 2004). The inclusion-free rims commonly observed surrounding poikiloblastic garnet cores may result from a late stage of slow growth or perhaps from a different garnet-forming reaction than the one that formed the cores.

Skeletal texture (also called **web**, or **spongy**) is an extreme example of poikiloblast formation (Figures 9i and 12), in which the inclusions form the bulk of the

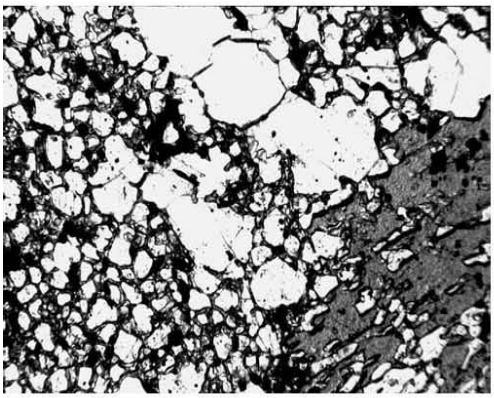

FIGURE 12 Skeletal or web texture of staurolite in a quartzite. The gray intergranular material, and the mass in the lower right, are all part of a single large staurolite crystal. Pateca, New Mexico. Width of view ~5 mm.

FIGURE 13 Light-colored depletion haloes around cm-sized garnets in amphibolite. Fe and Mg were less plentiful, so that hornblende was consumed to a greater extent than was plagioclase as the garnets grew, leaving hornblende-depleted zones. Sample courtesy of Peter Misch.

rock and the enclosing mineral phase occurs almost as an intergranular, crystallographically continuous, network. It may develop at the margins of some porphyroblasts where they are growing into the matrix, but the occurrence is more pervasive in some rocks. Skeletal texture may result from rapid poikiloblast growth or from the introduction of poikiloblast-building or reactive components via an intergranular fluid.

Porphyroblasts typically form in minerals for which nucleation is impeded. They are larger than the groundmass minerals and are separated by greater distances. Crystallizing groundmass minerals typically grow among preexisting grains and thus have little nucleation problem, whereas porphyroblasts must nucleate from scratch. Porphyroblast growth requires that components diffuse farther in order to add onto the growing porphyroblast surface. Perhaps poikiloblastic and skeletal texture are metamorphic equivalents of igneous dendritic quench textures in which the growing grain surface reaches out toward a source of components in cases where diffusion is slow. In many cases the distance that a critical component must travel may control the size of porphyroblasts. Once the distance becomes too great, porphyroblast growth ceases. Diffusion of components that are scarce in the area surrounding a growing porphyroblast may create a zone surrounding the porphyroblast that is depleted in those components. Such areas are called **depletion haloes** (Figure 13). Porphyroblasts tend to be larger at higher grade. Perhaps we can attribute this to less overstepping of the true reaction conditions at elevated temperature (hence subdued nucleation) combined with more effective diffusion.

Cordierite, biotite, and some other minerals commonly form ovoid porphyroblasts in contact aureoles, particularly when the matrix is very fine grained. The texture is called **nodular** (Figures 9f and 14a). A field term for rocks that in hand specimen contain small porphyroblasts (usually ovoid, but not necessarily so) in a fine matrix is **spotted**. If the matrix is non-foliated the rock is commonly called a **spotted hornfels**. Contact metamorphism overprinting regional metamorphism is common (reflecting either post-orogenic magmatism or the time required for magmas to rise to shallow regions following an orogenic metamorphic-plutonic event). The result for low-grade regional metamorphic rocks is **spotted slates** or **spotted phyllites** (Figure 14b).

You have probably noticed in the lab or in the field that some metamorphic minerals tend to be more euhedral than others. In contrast to igneous rocks, this capacity is no longer determined by which minerals grew earliest (early igneous minerals are surrounded by melt, so growth is unencumbered by contact with other minerals). Because all metamorphic minerals grow in contact with others, the tendency for a mineral to be more euhedral must then be a property of the mineral itself. Garnet and staurolite, for example, are typically euhedral, whereas quartz and carbonates tend to be anhedral. Crystals that develop good crystal faces have anisotropic surface energy that is high for some faces, but low for others, so that, when developed, the low-energy faces reduce the overall surface energy of the mineral. Rather than attempt a rigorous theoretical treatment, it is far simpler to create an empirical list of the common metamorphic minerals in terms of their tendency to form euhedral (idioblastic) crystals. Such a list has been available since Becke (1913) first proposed it as the "crystalloblastic series."

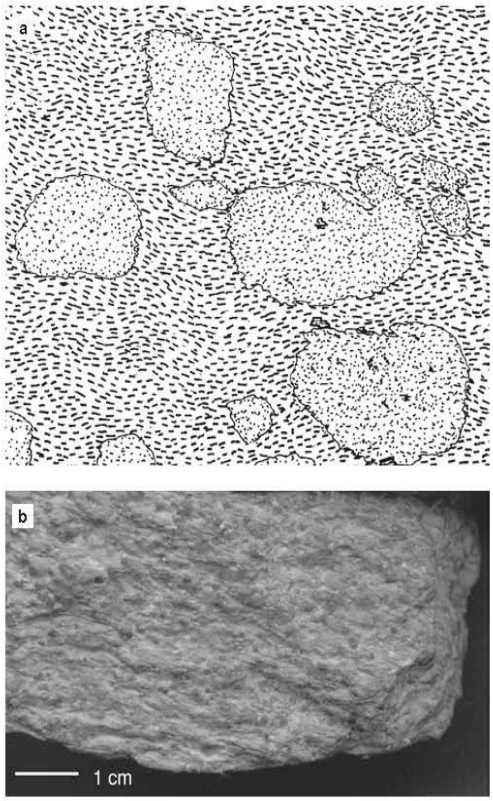

FIGURE 14 Overprint of contact metamorphism on regional. (a) Nodular texture of cordierite porphyroblasts developed during a thermal overprinting of regional metamorphism (note the foliation in the opaques). From Bard (1986), approximately 1.5 × 2mm. Copyright © by permission Kluwer Academic Publishers. (b) Spotted phyllite in which small porphyroblasts of cordierite (and one larger pyrite) develop in a preexisting phyllite.

THE CRYSTALLOBLASTIC SERIES

Most Euhedral

Titanite, rutile, pyrite, spinel
Garnet, sillimanite, staurolite, tourmaline
Epidote, magnetite, ilmenite
Andalusite, pyroxene, amphibole
Mica, chlorite, dolomite, kyanite
Calcite, vesuvianite, scapolite
Feldspar, quartz, cordierite

Least Euhedral

Porphyroblasts, even of the same mineral, may exhibit euhedral outlines in one rock and anhedral ones in another. As with igneous crystals, euhedral shapes are generally attributed to growth into a liquid rather than interference with adjacent solids. In metamorphic rocks, this may involve only a thin surface film of aqueous fluid, perhaps released by a prograde dehydration reaction in which the porphyroblast is one product (Vernon, 2004). Euhedral porphyroblasts are rare in dry high-grade metamorphic rocks, which supports this idea.

Cashman and Ferry (1988) plotted the number of grains as a function of grain size (called **crystal size distribution [CSD]** plots) for olivine, pyroxene, and magnetite in high-temperature hornfelses (~1000°C) from Skye. They found that CSDs for the hornfelses plot in a log-linear fashion with ever-increasing numbers of grains as crystal size decreases. This is the same pattern developed in volcanics, which Cashman and Ferry (1988) interpreted to reflect both continuous nucleation and growth that quickly cease due to cooling and kinetic constraints. As we shall see, the CSD patterns in many areas of *regional* metamorphism do not conform to this log-linear trend.

As metamorphic grade (mostly temperature) increases, recrystallization becomes more dominant. Thus we might summarize the following as the most pronounced *textural* effects of increasing metamorphic grade in contact aureoles:

1. Fewer relict textures and a more fully recrystallized metamorphic texture
2. Increased grain size
3. Straighter grain boundaries and less evidence of strain

3 HIGH-STRAIN METAMORPHIC TEXTURES

Because impacts are rare, we will concentrate here on fault/shear zones. In shallow fault zones where the rocks are cooler and behavior is more brittle, the cataclastic processes described in the beginning of Section 1 dominate over the recovery and re-crystallization processes. Broken, crushed, rotated, and bent grains dominate in fault breccias.

Below this shallowest zone, confining pressure increases, and deformation is more pervasive. Cataclastic processes continue to be dominant at intermediate depths, and affect the rock on a finer scale. The rocks are more coherent microbreccias and cataclasites. Phyllosilicates slip readily along (001) and may become disrupted by slip. The thin plates produced by slip easily bend or break, which produces a more frayed or **shredded** appearance at high strain rates. **Undulose extinction** is ubiquitous. Undulose extinction of deformed lattices in plagioclase may be distinguished from compositional zoning by the generally concentric extinction pattern of the latter. Remnants of broken larger pre-deformational grains are called **clasts** (from cata*clastic*). Larger initial grains (sedimentary grains or phenocrysts) or more resistant minerals may remain larger in a matrix of crushed material. These larger fragments are called **porphyro*clasts*** (to distinguish them from porphyro*blasts* that *grew* larger). Some porphyroclasts may be surrounded by a matrix of fine crushed material that is derived from them as they are rotated and ground down, a texture called **mortar** texture (Figure 15b). **Pseudotachylite** is produced by localized rapid fragmentation and melting due to shear heating, generally attributed to earthquake shock energy in dry rocks (Sibson, 1975; Vernon, 2004). Figure 16b shows the typical outcrop structure of pseudotachylite, with dark sharply

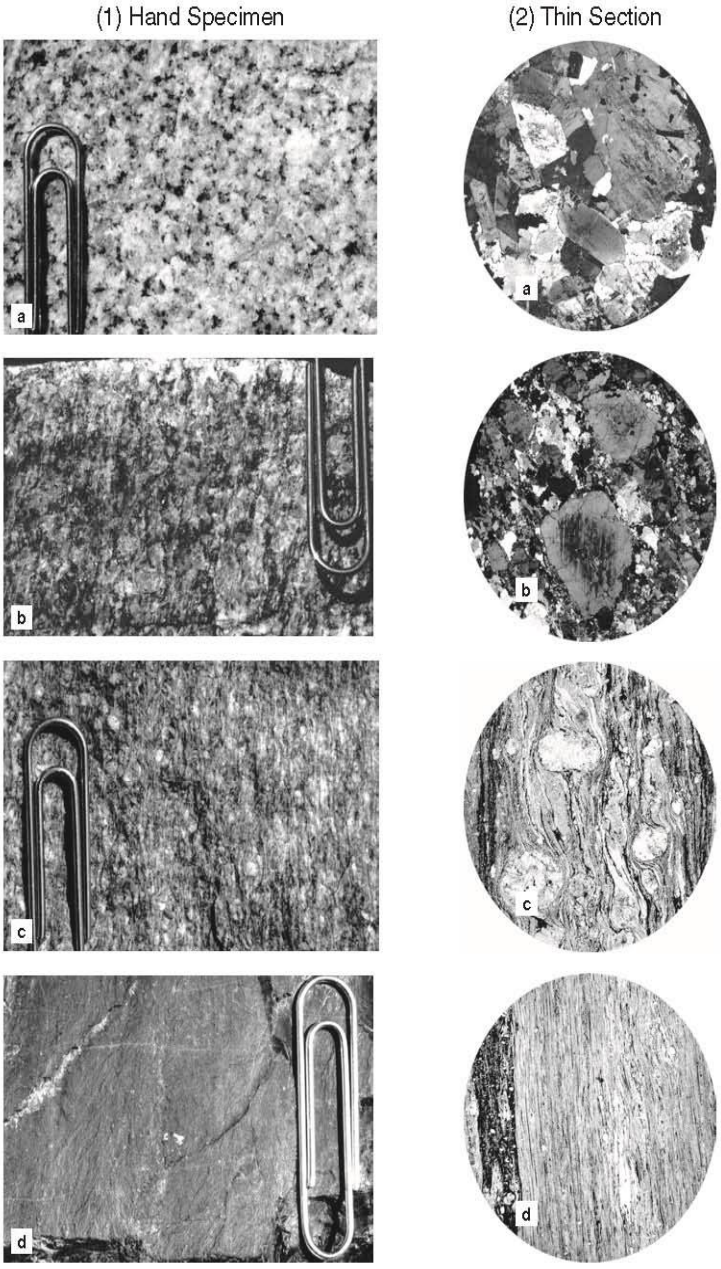

FIGURE 15 A series of four specimens (left) and photomicrographs (right, 10×) showing the progressive mylonitization of granitic rocks in the southeastern San Gabriel Mountains, California. (a) Undeformed granite. (b) Mortar texture in which large porphyroclasts of quartz are surrounded by a crushed matrix derived by cataclasis and recrystallization. (c) Mylonitization imparts a distinct foliation as shear and recrystallization causes elongated elements. (d) Ultramylonite, in which very little of the original grains remain. Ribbon texture predominates. © Shelton © (1966).

bounded irregular dendritic veins containing deformed grains suspended in a glassy matrix. Rapid cooling of the narrow veins preserves both the glass and the deformed textures. The name comes from tachylite (basaltic glass). Curiously, the melt composition is typically mafic, even when formed in more silicic rocks. Camacho et al. (1995), for example, reported the occurrence of pseudotachylite with a mafic glass composition that developed in felsic granulites (orthopyroxene meta-granitoids). Apparently, pyroxene and plagioclase structures are more easily disturbed by the shock than associated

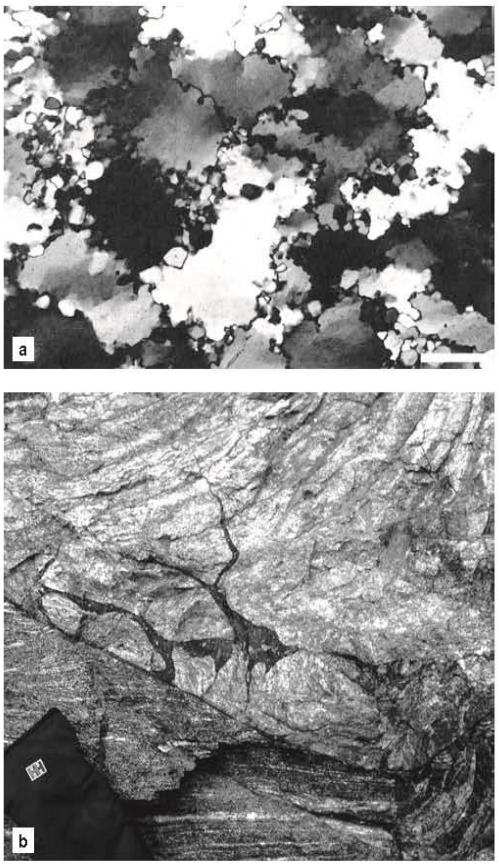

FIGURE 16 (a) Large polygonized quartz crystals with undulose extinction and subgrains that show sutured grain boundaries caused by recrystallization. From Urai et al. (1986 © AGU with permission). Compare to Figure 15b, in which little, if any, recrystallization has occurred. (b) Vein-like pseudotachylite developed in gneisses, Hebron Fjord area, northern Labrador, Canada.

quartz and K-feldspar so that the mafic component melted. This is an interesting example of high energy dynamics that produces partial melting trends that contrast sharply to equilibrium melting experiments we generally rely upon.

Shear zones typically broaden at depth so that shear is distributed and ductile processes gradually become more prevalent. Deformation occurs as a result of combined cataclastic, plastic intracrystalline deformation, and recovery processes. Twinned and ductilely elongated grains are common. Foliated **mylonites** are the predominant type of rock. Quartz may have the form of highly elongate **ribbons** (Figure 15c and d).

Foliations are important in the interpretation of mylonites, especially in determining the sense of shear motion in the shear zone (see below). Foliations occur in shear zones and in orogenic belts of regional extent. They are more varied in the latter, and I shall postpone discussing the types and generation of foliations until we address orogenic metamorphic textures in Section 4.

Recovery processes, even when dynamic and accompanying deformation, result in the formation of subgrains. Traditional descriptions of the formation of smaller reduced-strain subgrains and grains from larger deformed grains refer to the collective process as **polygonization**. Figures 16a and 4b are photomicrographs of polygonized quartz.

Recovery and recrystallization become progressively more important as deformation wanes. Highly deformed rocks have high strain energy and tend to recrystallize readily. Grain boundary migration and subgrain rotation result in serrated-sutured boundaries (Figure 16a). If the temperature is high enough, recrystallization may progress further, and serrated boundaries become coarser and less sharply curved (Figure 7a), and the shapes of the larger crystals appear more **amoeboid**. In cases of advanced recrystallization, grain boundary area reduction straightens the boundaries further, eventually producing a granoblastic polygonal texture that is completely recrystallized (annealed). The collective process by which larger grains form from subgrains or by the addition of smaller grains by grain boundary migration recrystallization has been traditionally referred to as **coalescence**.

3.1 Shear Sense Indicators

In order to properly interpret deformation, it is useful to know the sense of shear between opposing blocks across a fault zone that is no longer active. Plate tectonics has increased our interest in knowing the sense of shear, as it may help us to determine the relative motions of crustal blocks involved in orogeny. The *direction* of motion in a shear zone is in the shear zone plane and assumed to be parallel to fault striations or mineral elongation. The *sense* of shear (which of the two opposite possible motions associated with a given direction), however, is more difficult to determine. It is important to understand shear offset in three dimensions, as the sense of offset on a two-dimensional surface may be misleading if the direction of motion has not clearly been determined. Orientation of samples is critical, and it will be assumed in the following discussion that we are observing textures in a direction that is both *in the shear plane and normal to the direction of motion*. In the figures that follow, the shear plane will thus be normal to the page and the direction of shear will be right–left (and the sense will consistently be dextral (clockwise). Proper orientation may be difficult to manage on two-dimensional outcrops in the field but can be accomplished by cutting thin sections from appropriately reoriented hand specimens.

If a planar or linear structure is cut by the shear plane, we can use the offset or drag-curvature features to easily determine the sense of offset (as in the dark dikelet in Figure 17a, top, or the foliation in Figure 8). Many shear zones, however, do not show foliations that curve into them, at least not on the outcrop or smaller scale. When offset or curved markers are absent, careful textural analysis and interpretation are required.

Oblique foliations, such as those developed in the schematic quartz grains of Figure 17a, cut across an S-foliation developed as shear offsets. To understand the two

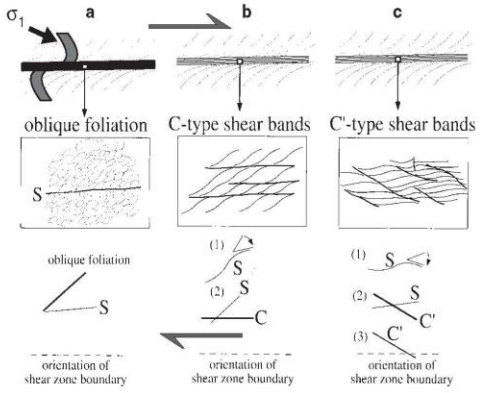

FIGURE 17 Some features that permit the determination of sense of shear. All examples involve dextral shear. σ_1 is oriented as shown. **(a)** Passive planar marker unit (shaded) and foliation oblique to shear planes. **(b)** S-C foliations. **(c)** S-C′ foliations. σ_1 is the direction of maximum principal stress. After Passchier and Trouw (2005). Copyright © with permission from Springer-Verlag.

sets of foliations, consider a deck of cards. If we shear the deck (slip between the individual cards), any material in the volume being sheared (such as a line or circle drawn on the side of the deck) will elongate and rotate to define a foliation. The shear planes (between cards) define another foliation. With progressive shear, the two foliations approach one another, but can never become truly parallel. The foliation labeled S in Figure 17a is the card-parallel shear foliation and the oblique foliation is the stretching (long axis) of the material elements. The quadrants with the *acute* angle between the S-foliation and the oblique foliation indicate the shear sense direction.

Shear bands (labeled C in Figure 17b) are spaced cleavages that transect a well-developed simultaneous mineral foliation (S in Figure 17b) at a small angle. The combined texture is called **shear band cleavage** or **S-C** texture. Mylonites showing shear band cleavage are called **S-C mylonites** (Berthé et al., 1979; Lister and Snoke, 1984). The C-type surfaces are parallel to the main shear zone offset, and the sense of shear is determined by the acute angle between the S and C foliations. A **C′-type** of cleavage may also form in some instances, usually later than the S- and C-types (Figure 17c). C′ is oriented in a *conjugate* sense to the C-type cleavage (σ_1 bisects the acute angle between them), so it is oblique to the shear zone boundaries (by 15 to 35°). C′-type cleavages are usually more weakly developed, shorter, and more wavy than C-types.

Porphyroclasts developed in sheared mylonite typically develop tapered rims of fine-grained material. If the rims have the same mineralogy as the porphyroclast, they are assumed to be derived from the porphyroclast by grinding and are called **mantles**. **Mantled porphyroclasts** typically develop from more resistant feldspars in a matrix of quartz, feldspar, and mica in sheared granites, or from dolomite in sheared calcite–dolomite marbles. Mantles are interpreted to form by ductile crystal deformation and storage of dislocation tangles in the rim of porphyroclasts in response to flow in the matrix. The rim then recrystallizes to form the mantle. Coarse **augen** texture in mylonites and more ductile sheared granitic gneisses (Figure 18) are types of mantled porphyroclasts. The mantle is finer grained than the porphyroclast core and can be further deformed by shear to form **tails** that extend from the porphyroclast in both directions into the mylonitic foliation (Vernon, 2004).

The shape of the deformed tails on *some* mantled porphyroclasts can be used as shear-sense indicators. Mantled porphyroclasts can be subdivided into five types (Simpson and Schmidt, 1983; Simpson, 1985; Passchier and Simpson, 1986; Passchier and Trouw, 2005). As illustrated in Figure 19, **θ-type** mantles have no tails, and **ϕ-type** mantles have symmetrical tails. Neither can be used as sense-of-shear indicators. **σ-type** mantled porphyroclasts are asymmetrical and have wide tails, with a nearly straight outer side. The inner side is usually concave toward the median plane (the plane parallel to the shear zone and bisecting the porphyroclast). The shape has been described as **stair-step** because the two outer sides offset in two directions, just like the rise and run of a stair. The tail shape is believed to form as the foliation drags the softer mantle. The stair-step can be used to infer the sense of shear as illustrated for the σ-type in Figure 19.

In **δ-type** mantled porphyroclasts, both sides of the mantle are curved, and an embayment is formed on the inner side. δ-types are believed to begin as σ-types, and the curvature probably forms as the core rotates during further shear. The shape is related to the median plane and sense of shear as illustrated in Figure 19. Care must be taken when interpreting sense of shear from δ-type and σ-type mantled porphyroclasts. Note that if you mentally straighten the curvature of the δ-type tails in Figure 19, it looks like an σ-type, *but if improperly interpreted as σ-type, the sense of*

FIGURE 18 Augen gneiss with eye-shaped porphyroclasts (augen) of K-feldspar in a sheared granitic matrix.

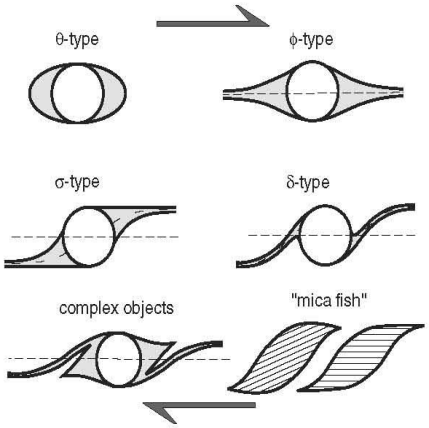

FIGURE 19 Mantled porphyroclasts and "mica fish" as sense-of-shear indicators. After Passchier and Simpson (1986). Copyright © with permission from Elsevier Science.

shear it then indicates is opposite the true sense. You must therefore be certain of the type of porphyroclast that you are observing before you can interpret it correctly.

Complex object mantled porphyroclasts are generated by further rotation of δ-types, which again stretches out the mantle in a renewed σ-type fashion. By using the shape in Figure 19, the sense of shear can be determined.

"Mica-fish" are single mica crystals (not porphyroclasts) that are shaped much like σ-type mantled porphyroclasts (Figure 19). They are most common in mica–quartz mylonites and ultramylonites. Like σ-type porphyroclasts, their long axis is oriented in the direction of extension (see below). This and the "stair-step" form can be used to indicate sense of shear. The mica {001} cleavages may be parallel to the elongation direction, or they may be oriented parallel to the slip direction of the shear zone (as shown in the two examples in Figure 19). Trails of mica fragments typically extend from the tips well into the matrix. Lister and Snoke (1984) proposed that mica-fish form by a combination of slip on {001}, rotation, boudinage (see below), and recrystallization at the edges.

Other sense-of-shear indicators (Figure 20) include **quarter structures** that form on unmantled porphyroclasts. Quarter structures are so named because the four quadrants defined by the foliation and its normal are not symmetrical. In Figure 20, for example, the northwestern and southeastern quadrants experience shortening, and the northeastern and southwestern ones experience extension. In **quarter folds** (Figure 20a), shear extension drags small folds in the foliation around porphyroclasts. **Quarter mats** (Figure 20b) are concentrations of mica that result from dissolution of quartz in the shortened quadrants and precipitation in the extending quadrants. The vergence of **asymmetric folds** (Figure 20c) is also a good shear-sense indicator, as are pairs of pre-shear dikelets if one is in the quadrants of extension and the other in the quadrants of compression (Figure 20d). Other shear-sense indicators may also be used, but most are either more cumbersome, more specialized, or inconsistent.

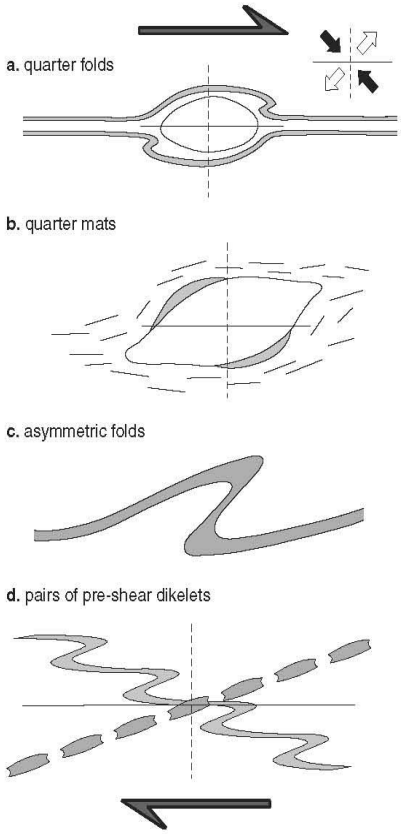

FIGURE 20 Other methods to determine sense of shear.

See Passchier and Trouw (2005) and Vernon (2004) for detailed discussions of shear-sense indicators.

4 REGIONAL OROGENIC METAMORPHIC TEXTURES

The textures discussed in this section are appropriately called **dynamothermal** textures because they occur in any situation where deformation and heat are combined. Such situations range from deep shear zones to strained contact aureoles, but the majority of dynamothermal rocks are found in ancient orogenic belts, so we will concentrate on this setting.

Orogenic belts are complex tectonic environments where plate convergence produces a number of deformational and thermal patterns. We can envision an **orogeny** as a long-term mountain building process, such as the Appalachian Orogeny or the Alpine Orogeny. Orogenies are not continuous, however, and an orogeny may comprise more than one **tectonic event**, believed to result most commonly from short-term changes in plate motion, such as accelerated subduction rate or (micro)- continent accretion. Tectonic events, in turn, may consist of more than one **deformation phase**. A deformation phase, according to Passchier and Trouw (2005), is a distinct period of active deformation with a specific style and orientation.

Deformation phases may be separated by periods of reduced or absent deformation, during which the orientation of the stress field may change. Thus one or more deformation phases may constitute a tectonic event, and one or more tectonic events may constitute an orogeny.

Metamorphism accompanies many of these deformational processes but not necessarily in a direct one-to-one manner. We might best consider metamorphism separately as occurring in one or more **metamorphic reaction events** that in turn occur in a larger **metamorphic cycle** (in which rocks are buried, heated, metamorphosed, and then brought back to the surface by uplift and erosion). There may also conceivably be more than one metamorphic cycle in an orogeny. Metamorphic events typically last 1 to 10 Ma, but multiple events in an orogen may span over 1 Ga. Metamorphism may accompany only some deformational events, and the style of deformation and grade of metamorphism may vary in both time and space within a single orogen. A single metamorphic event may even have more than one **phase** of heating within it. The IUGS-SCMR (Fettes and Desmons, 2007) proposed the term **polyphase** for a broad *P-T-t* cycle (event) with more than one temperature climax (phases). **Monophase** metamorphic events have only one climax. **Polymetamorphic** is a term that describes more than one event.

Deformation tends to break minerals down to smaller grains and subgrains, whereas the heat of metamorphism tends to build them back up again. Such a complex set of processes allows for myriad interactions and overprints between metamorphic mineral growth and deformation, making the study of textures in orogenic rocks a challenge and often leading to controversy over textural interpretations. Of course, whenever things get complex, there is more useful information to be gathered, so complexity becomes a benefit when the features can be interpreted properly. We can do a respectable job on the basis of a few guiding principles. In the following summary, I review the useful principles upon which geologists tend to agree and discuss some of the remaining controversial aspects of the textural interpretation of orogenically metamorphosed rocks.

As I alluded to above, the crystal size distribution (CSD) curves for regional metamorphism differ from those of contact metamorphism. In contrast to the log-linear plots for contact metamorphism (and volcanics), Cashman and Ferry (1988) found that regional CSDs have a bell-shaped pattern. The grain size of the maximum of the CSD curves increases with grade, as we would expect. Cashman and Ferry (1988) attributed the bell shape to initial continuous nucleation and crystal growth (as in contact rocks) followed by a period of annealing in which nucleation ceases and larger grains grow at the expense of smaller ones (as in Ostwald ripening). The minimum grain size in regional metamorphism thus appears to reflect continued growth after nucleation ends.

4.1 Tectonites, Foliations, and Lineations

A **tectonite** is a deformed rock with a texture that records the deformation by developing a preferred mineral orientation of some sort. The fabric of a tectonite is the complete spatial and geometrical configuration of its textural and structural elements. **Foliation** is a general term for any planar textural element in a rock, whereas **lineation** similarly applies to linear elements. Foliations and lineations can be subdivided into **primary** (pre-deformational) ones, such as bedding, and **secondary** (deformational) ones. Minerals may be oriented by either dimensional preferred orientation (DPO) or lattice preferred orientation (LPO), or both. Although they are treated separately, there is probably a complete natural gradation from pure foliations through combined foliations and lineations to pure lineations.

4.1.1 FOLIATIONS. A number of features can define a secondary foliation (Figure 21), including platy minerals, linear minerals, layers, fractures, and flattened elements.

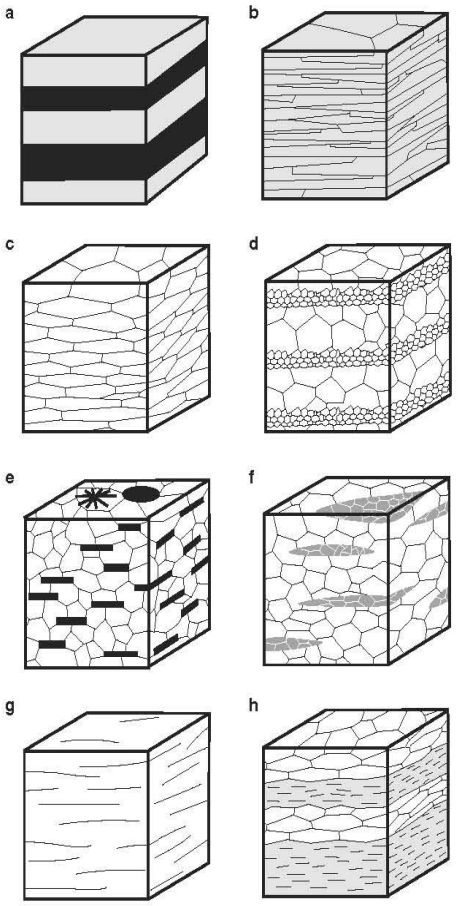

FIGURE 21 Types of fabric elements that may define a foliation. **(a)** Compositional layering. **(b)** Preferred orientation of platy minerals. **(c)** Shape of deformed grains. **(d)** Grain size variation. **(e)** Preferred orientation of platy minerals in a matrix without preferred orientation. Note that linear minerals may also define a foliation if randomly oriented in a plane. **(f)** Preferred orientation of lenticular mineral aggregates. **(g)** Preferred orientation of fractures. **(h)** Combinations of the above. From Turner and Weiss (1963) and Passchier and Trouw (2005).

Metamorphic foliations are divided into cleavages (fine penetrative foliations), schistosity (coarser penetrative foliations), and gneissose structure (poorly developed coarse foliations or segregated layers). The nomenclature of **cleavages** suffers from an overabundance of terms that were used in different ways by different investigators and often confused the purely descriptive from the genetic aspects. A Penrose Conference was held in 1976 to reach a consensus on the description and origins of rock cleavages (Platt, 1976). Although consensus was not immediately forthcoming, Powell (1979) followed it up and proposed a classification of cleavages (including schistosity) that was purely descriptive, thereby allowing us a universal nomenclature unencumbered by inferences about cleavage origins.

Geological processes are usually slow, and the majority of petrological phenomena that we see today have remained unchanged since scientists first observed them. Interpretations as to the origin of the features, on the other hand, change often as new ideas and data come to light. Thus it is always a good idea to separate our observations from our interpretations, so that we may speculate freely after we have agreed upon what we see. Powell's (1979) classification has thus met with approval from the majority of investigators in the field and is presented in Figure 22,

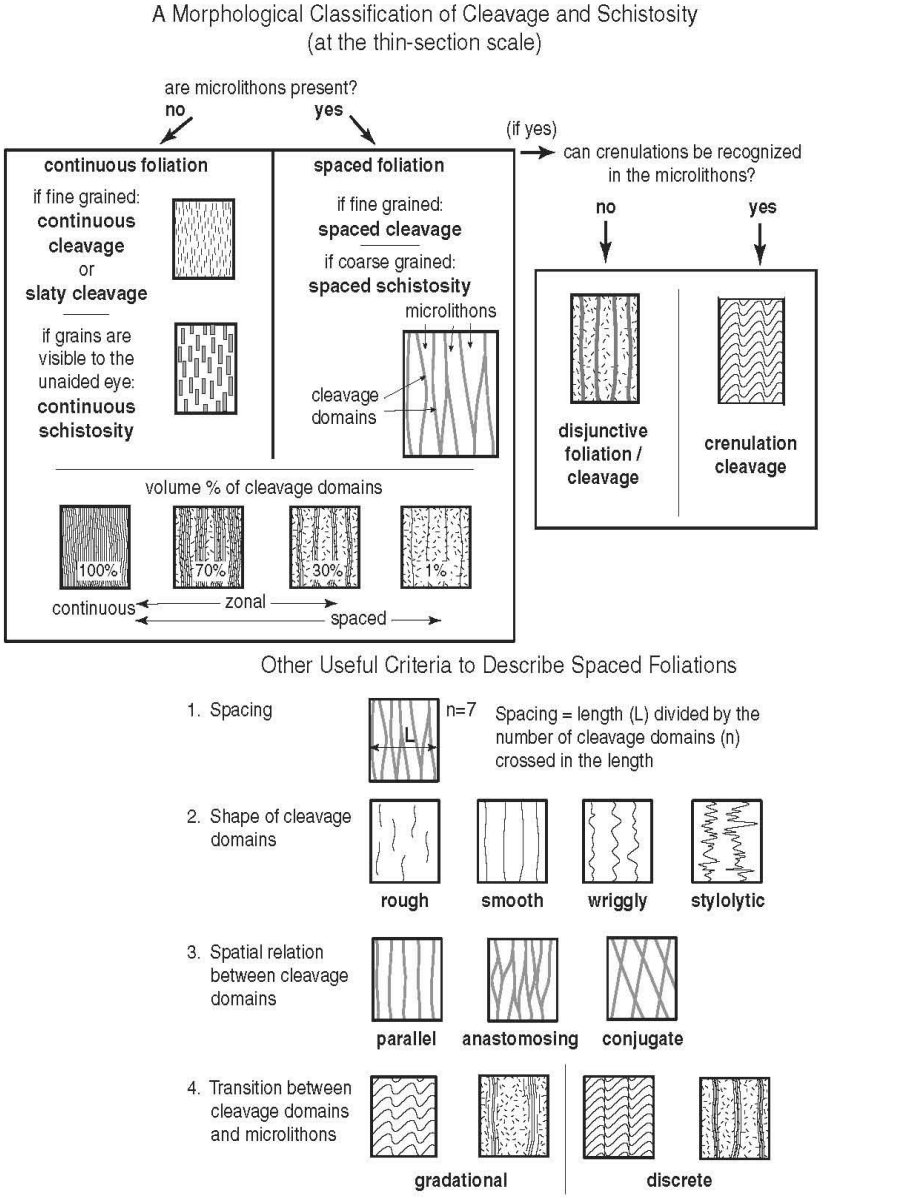

FIGURE 22 A morphological (non-genetic) classification of foliations. After Powell (1979), Borradaile et al. (1982), and Passchier and Trouw (2005).

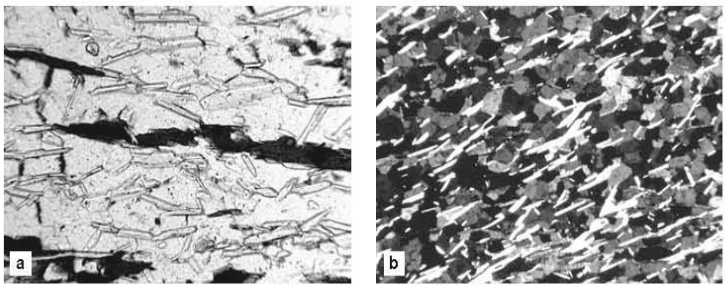

FIGURE 23 Continuous schistosity developed by dynamic recrystallization of biotite, muscovite, and quartz. (a) Plane-polarized light, width of field 1 mm. (b) Another sample with crossed-polars, width of field 2 mm. Although there is a definite foliation in both samples, the minerals are entirely strain free.

as modified slightly by Borradaile et al. (1982), Passchier and Trouw (2005), and me. The description of cleavages in some cases may be done in hand specimen, but it is best done with the aid of thin sections. Figure 22 is thus based largely on thin section–scale features.

The first step in characterizing a cleavage is to decide whether the foliation elements are *continuous* or *spaced*. In a **continuous foliation**, the aligned minerals define a foliation that does not vary across the area of the thin section (Figure 23). In a **spaced foliation**, the fabric of the rock is separated into unfoliated **microlithons** separated by **cleavage domains** (fractures or concentrations of platy minerals). Of course, there is a continuum between these idealized end-members, and continuous cleavage grades through zonal to spaced cleavage (Figure 22). Fine-grained continuous cleavage may also be called **slaty cleavage** because it typifies slates. As Vernon (1998, 2004) pointed out, however, slates may develop some degree of spacing into anastomosing lenticular P-rich and Q-rich domains (Section 4.3), even at very low grades. Most petrologists still refer to such finely spaced cleavages as slaty cleavage. Phyllites have a slightly coarser continuous cleavage, and, when the individual aligned crystals become large enough to see with the unaided eye, the foliation is called a **schistosity**.

Spaced foliations are further subdivided and described on the basis of the spacing and shape of the cleavage domains, the presence of crenulations, the spatial relations between the domains, and whether the domains grade into the microlithons. These characteristics are also illustrated in Figure 22. Terms that describe these aspects may be combined when appropriate (e.g., a "smooth, anastomosing, discrete cleavage," etc.).

A **crenulation cleavage** is actually *two* cleavages. The first cleavage may be a slaty cleavage or schistosity that becomes microfolded. The fold axial planes typically form at a high angle to σ_1 of the second compressional phase. The folds may be *symmetrical* (Figure 24a) or *asymmetrical* (Figure 24b). Quartz grains tend to dissolve by pressure solution from the fold limbs (or just the steeper limb of asymmetrical folds) either to precipitate in the hinge areas or be transported further away (Figure 24). If the metamorphic temperature is high enough, new micas may also grow normal to σ_1 during the second phase. Pressure solution and the growth of new minerals may both enhance the second foliation and obscure the first, as can be seen in the sequence $1 \rightarrow 5$ in Figure 25. In such cases, the first foliation is most evident in the microlithons between the second cleavage (see also Figures 24a, 42, and 48b).

Compositional **layering** is a common type of foliation that can be either primary or secondary. Primary layering, such as bedding, cumulate layering, or igneous flow features, is inherited from the pre-metamorphic rock. A common form of secondary layering is **gneissose structure**. We shall discuss metamorphic layering in more detail below.

4.1.2 LINEATIONS. Foliations generally occur when $\sigma_1 > \sigma_2 \approx \sigma_3$ and lineations generally occur when $\sigma_1 \approx \sigma_2 > \sigma_3$, or when shear smears out an object. As shown in Figure 26, there are also several types of lineations. They usually result from the elongation of minerals or mineral aggregates (**stretching lineations**). Stretched pebbles in deformed conglomerates is a common example. Lineations may also result from parallel **growth of elongate minerals**, **fold axes**, or **intersecting planar elements** (cleavage and bedding, or two cleavages). Note in Figure 26c that, under some circumstances, *planar* minerals can create a *linear* fabric, just as *linear* minerals can create a *planar* fabric in Figure 21e.

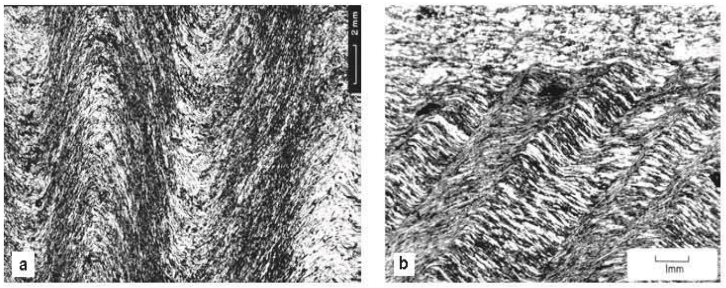

FIGURE 24 Crenulation cleavages. (a) (top) Symmetrical crenulation cleavages in amphibole–quartz-rich schist. Note concentration of quartz in hinge areas. (b) Asymmetric crenulation cleavages in mica–quartz-rich schist. Note horizontal compositional layering (relict bedding) and preferential dissolution of quartz from one limb of the folds. From Borradaile et al. (1982).

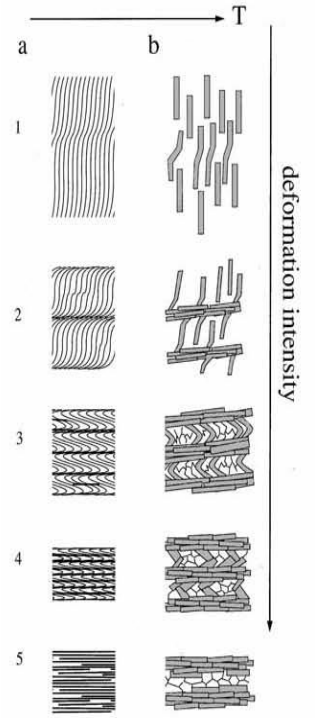

FIGURE 25 Stages in the development of crenulation cleavage as a function of temperature and intensity of the second deformation. From Passchier and Trouw (2005). Copyright © with permission from Springer-Verlag.

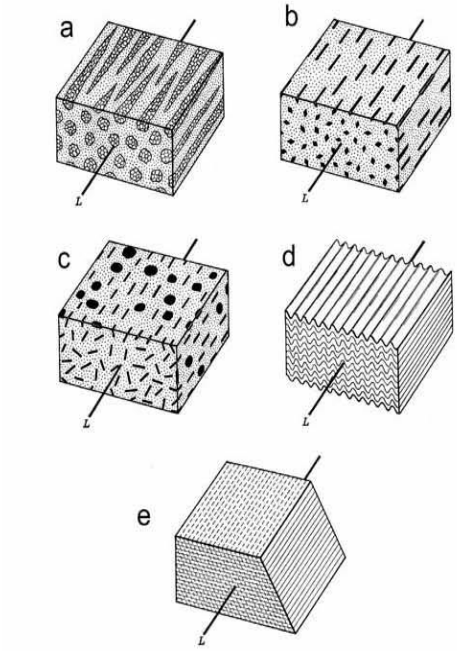

FIGURE 26 Types of fabric elements that define a lineation. (a) Preferred orientation of elongated mineral aggregates. (b) Preferred orientation of elongate minerals. (c) Lineation defined by platy minerals. (d) Fold axes (especially of crenulations). (e) Intersecting planar elements. From Turner and Weiss (1963). Copyright © with permission of the McGraw Hill Companies.

4.2 Mechanisms of Tectonite Development

Secondary (metamorphic) fabric elements in regionally metamorphosed rocks develop in response to deformation ± mineral growth. We shall concentrate on foliations here, but lineations are created in a similar fashion, depending largely on the relative magnitudes of σ_1, σ_2, and σ_3. Figure 27 illustrates the principal ways that we presently think a foliation may develop in a rock. How a rock or a mineral grain responds depends upon the type of mineral, pressure, temperature, magnitude and orientation of the stress field, and composition and pressure of the fluid. For reviews of the mechanisms by which foliations develop, see Shelley (1993) or Passchier and Trouw (2005) and the references therein.

Mechanical rotation (Figure 27a) may already be familiar to you. The minerals behave as fairly rigid objects, although some minerals may deform internally by cataclasis during rotation. This mechanism occurs in low-temperature areas, such as shallow shear zones and low-temperature regional metamorphics.

Oriented new mineral growth involves either nucleation or preferred growth of existing minerals in advantageous orientations (Figure 27b and c). Many minerals grow most readily in directions in which the compression is least, and thus platy minerals typically grow normal to σ_1 and columnar or accicular minerals grow elongated parallel to σ_3. Existing minerals that are elongated in the direction of σ_1 may not grow at all or may even dissolve and become shorter (Figure 27c). Favorably aligned minerals may thus grow at the expense of unfavorably aligned ones. This process has been called **competitive growth**.

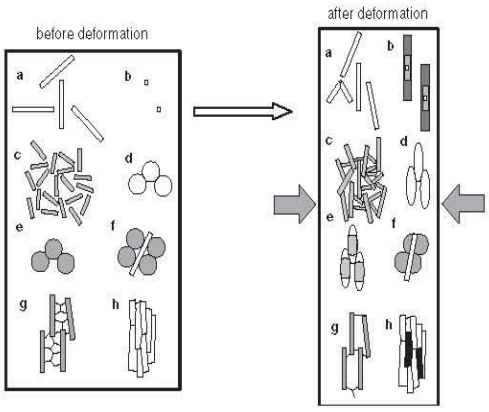

FIGURE 27 Proposed mechanisms for the development of foliations. (a) Mechanical rotation. (b) Preferred growth normal to compression. (c) Grains with advantageous orientation grow whereas those with poor orientation do not (or dissolve). (d) Minerals change shape by ductile deformation. (e) Solution transfer. (f) A combination of (a) and (e). (g) Constrained growth between platy minerals. (h) Mimetic growth following an existing foliation. After Passchier and Trouw (2005). Copyright © with permission from Springer-Verlag.

Crystal-plastic deformation and recrystallization may also result in elongated minerals during shear or flattening (Figures 27d). Figure 28 illustrates the development of continuous mineral foliations by both processes. Flattening causes the foliation to be elongated normal to σ_1 which parallels the shortest axis of the strain ellipsoid. Shear, as discussed in conjunction with Figure 17, rotates a preexisting foliation toward the direction normal to the shortest axis of the strain ellipsoid, but it never reaches it. Note in Figure 28c that, if the initial state is already foliated as shown, flattening will enhance the foliation in its original orientation, and shear will *reorient* it. The reorientation of a foliation by folding or shear is called **transposition**.

Minerals such as quartz, which tends to be equidimensional in metamorphic rocks, even under conditions of regional metamorphism, may deform to elongated (Figure 29) or even **ribbon** shapes by crystal plastic mechanisms in mylonites (Figure 15d).

Solution transfer (Figures 27e and f), discussed earlier in conjunction with Figure 1, can produce elongated mineral shapes or enhance other foliations by dissolving minerals from high-pressure areas (surfaces at a high angle to σ_1). Loss of quartz from the limbs of folds (Figure 24) makes the mica foliation much more evident, as does removing carbonate or quartz, to leave an insoluble residue that defines a cleavage domain. Solution all but requires the presence of a fluid.

Mineral elongation and parallel growth may also occur in a passive sense. For example (as described earlier), quartz may become elongated due to constraints imposed by neighboring oriented mica grains. Thus in Figures 11 and 27g the increase in grain size of recrystallizing quartz is confined by the aligned micas and the stability of the mica {001} faces. Thus the quartz crystals develop a dimensional preferred orientation (DPO) as they conform to the micas. **Mimetic** mineral growth is also a common phenomenon that can produce oriented minerals even under nearly lithostatic stress conditions. If, for example, dynamic crystallization produces a preferred orientation of mica in a schist, and that schist is recrystallized during a later non-deformational thermal event, static mica growth during the annealing event ought to be random. Recrystallization, however, may be easier by conforming to the preexisting micas. Other minerals may also conform, either by epitaxial nucleation of new minerals or due to restrictions on growth imposed by neighboring mica grains. Thermodynamic (chemical and mineralogical) equilibrium is usually established before textural equilibrium. Thus textural equilibrium is particularly dependent upon the length of time that a rock is maintained at high temperature.

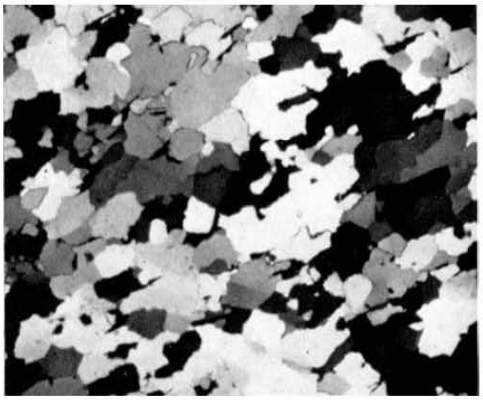

FIGURE 29 Deformed quartzite with elongated quartz crystals following shear, recovery, and recrystallization. Note the broad and rounded suturing due to coalescence. Field width ~1 cm. From Spry (1969).

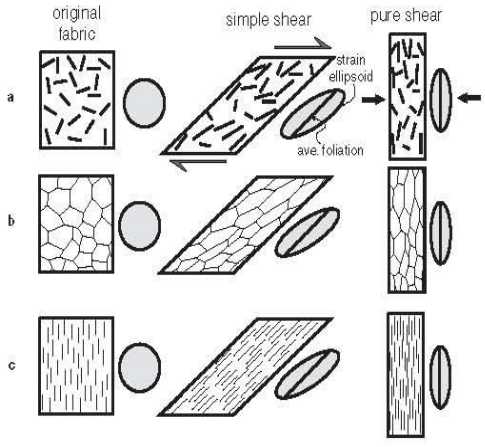

FIGURE 28 Development of foliation by simple shear and pure shear (flattening). (a) Beginning with randomly oriented planar or linear elements. (b) Beginning with equidimensional crystals. (c) Beginning with preexisting foliation. Shaded figures represent an initial sphere and the resulting strain ellipsoid. After Passchier and Trouw (2005). Copyright © with permission from Springer-Verlag.

4.3 Gneissose Structure and Layers

Gneissose structure is either a secondary layering in a metamorphic rock or a poorly developed schistosity in which the platy minerals are dispersed. Gneissose structure can range from strongly planar to strongly linear. Fabric elements range from nearly continuous layers to discrete lensoidal shapes.

Several metamorphic rock types exhibit layers or lenses on the centimeter to several millimeter scale, and in gneisses it is practically characteristic. Such layering in fine-grained, low-grade rocks is generally relict bedding or igneous layering because secondary separation into contrasting layers requires diffusion, which is most effective at elevated temperature. Shear separation onto P-rich and Q-rich domains (see below) in slates and phyllites is an exception (although typically much finer). Also the layers in some schists may be small locally derived veins, typically quartz or calcite. Shear may transpose these veins so that they become nearly parallel to the schistosity.

Layers in higher-grade schists and gneisses appear to develop in initially unlayered rocks, and the layering is

attributed to a poorly defined processes collectively called **metamorphic differentiation** (Stillwell, 1918). Metamorphic differentiation runs contrary to the concept of increasing entropy with temperature, and processes that cause initially dispersed constituents to segregate into contrasting layers of more uniform composition and mineralogy are therefore interesting. Numerous mechanisms have been proposed, but it is still uncertain what is responsible. Proposals include solution transfer and redeposition via an aqueous phase (governed perhaps by local pressure gradients), local melt segregation, diffusion-controlled mineral development, and segregation of minerals as a result of their response to shear or stress differences (Stephens et al., 1979). Schmidt (1932) first proposed that micas segregate into high-shear areas due to their ability to slip readily on {001} cleavages, leaving quartzofeldspathic layers between the high-shear domains. Robin (1979) proposed a similar mechanism in which a layered muscovite-quartz ("M-Q") rock would develop an unequal distribution of differential stress $(\sigma_1 - \sigma_3)$, which would be higher in the less competent "M-rich" layers (now popularly called **P-rich**, for phyllosilicate), and that this would create localized pressure gradients. The pressure gradients cause unequal pressure solution and migration of matter to the low-stress (**"Q-rich"**) layers (solution transfer). SiO_2 is more mobile than Al_2O_3, so quartz–muscovite segregation becomes enhanced with time. The process, Robin argued, can be initiated by relatively small initial inhomogeneities. As mentioned earlier, segregation into fine P-rich and Q-rich domains may even occur at very low metamorphic grades in slates. Perhaps all the mechanisms proposed above are possible, and each occurs in one rock or another. For summaries of metamorphic differentiation, see Hyndman (1985), Shelley (1993), Kretz (1994), or Vernon (2004).

4.4 Other Regional Metamorphic Textures

Other textural and structural elements that may develop in deformed rocks and minerals are **folds** and **kink bands** (Figure 30). **Boudinage** is a process in which elements such as dikes or elongate minerals that are less ductile than their surroundings, stretch and separate into tablets or sausage shapes (called **boudins**, French for "sausages") as the surroundings deform by ductile flow (Figures 20d, 34e, and 36).

Proper study of tectonites usually requires that the hand specimen and thin section can be spatially related to the outcrop. This way, we can use our textural observations to estimate the local or regional stresses. **Well-oriented samples** are thus required. Techniques for collecting and recording oriented samples are described by Passchier and Trouw (2005). Laboratory work for lattice-preferred orientations (LPO) requires a **universal stage** that permits a petrographer to orient a crystal in a thin section in three dimensions and to record the spatial orientation of the crystal axes. See Turner and Weiss (1963), Emmons (1943), or Passchier and Trouw (2005) for universal stage techniques. The orientation of a sound statistical sampling of crystal axes can then be plotted on an equal-area stereonet, and the density distribution of points can be contoured to produce **petrofabric diagrams**. The two petrofabric diagrams in Figure 31 will be familiar to students of structural geology, who use similar diagrams for fold axes, etc. See Turner and Weiss (1963) or Passchier and Trouw (2005) for further information on petrofabric diagrams.

4.5 Deformation Versus Metamorphic Mineral Growth

Following the lead of Sander (1930, 1950) and Turner and Weiss (1963), foliated rocks are called **S-tectonites**, and we can refer to the foliations as **S-surfaces** (as a shorthand notation: **S**). Linear elements are **L-tectonites** (shorthand: **L**). If two or more geometric elements are present, we can add a numeric subscript to denote the *chronological* sequence in which they were developed and superimposed. S_0 and L_0 are reserved for primary structures, such as relict bedding or igneous layering, etc. S_1, S_2, S_3, etc. are then subsequently developed foliations, whenever present. Similarly, L_1, L_2, and

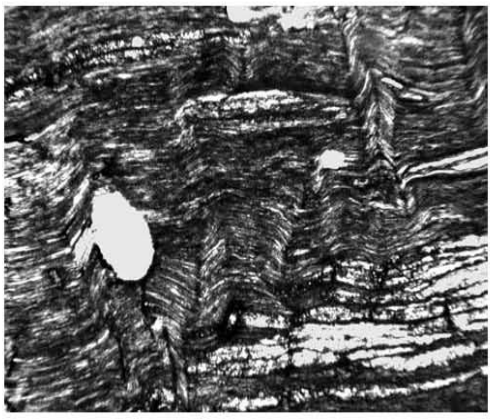

FIGURE 30 Kink bands involving cleavage in deformed chlorite. Inclusions are quartz (white), and epidote (lower right). Field of view ~1 mm.

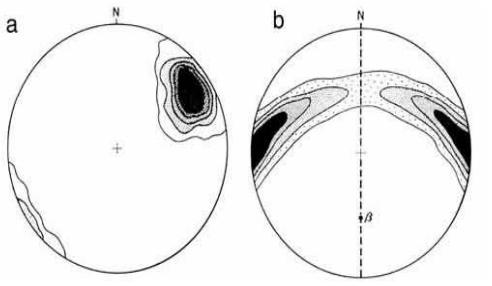

FIGURE 31 Examples of petrofabric diagrams. (a) Crystal c-axes cluster in a shallow inclination to the northeast. (b) Crystal axes form a girdle of maxima that represents folding of an earlier LPO. Poles cluster as normal to fold limbs. β represents the fold axis. The dashed line represents the axial plane and suggests that σ_1 was approximately east-west and horizontal. From Turner and Weiss (1963). Copyright © with permission of the McGraw-Hill Companies.

L_3 are successive secondary linear elements. By using this notation we can conveniently describe the sequential development of fabric elements in a tectonite. D_1, D_2, D_3, etc. can be used to refer to deformational phases, and M_1, M_2, M_3, etc. to metamorphic events so that we can then relate fabric elements and the minerals involved to the events that created them, provided of course that we can determine the relationships on the basis of textures. We cannot always figure out every detail of a rock's deformational and metamorphic history because some rather special textures are required to have developed, and later events may obscure evidence of earlier ones. Nonetheless, careful observation can often reveal a number of important textural clues. Also note that only the *relative* sequence of events is recorded petrographically, and *absolute* ages for multiple events require detailed isotopic work combined with structural–sedimentological–paleontological studies (Section 7).

As an example of the petrographic technique, suppose we begin with a pelitic sediment that has fine laminations of more sand-rich and clay-rich bedding (left and right halves of Figure 32). We conventionally call this primary foliation S_0. Suppose the sediment then becomes buried and metamorphosed (M_1) at some later date, and deformation (D_1) during the metamorphic event produces an excellent continuous cleavage in the metamorphic rock, which we then call S_1 (the sub-vertical foliation in Figure 32). S_1 is commonly subparallel to S_0 because the weight of the overlying strata causes a considerable vertical stress component on the originally horizontal bedding. Pelitic sedimentary rocks that have become compressed but not strongly deformed or metamorphosed may develop a **bedding-plane foliation** in which original clays or micas rotate in response to compaction. But horizontal compression is also a common facet of orogenic metamorphic events, and this adds a component of stress that reorients σ_1 a little from true vertical. This and later folding of S_0 causes S_1 to form most commonly at an angle to S_0 in the average thin section (although the angle may be quite small, as in Figure 32). This S_1 tends to obliterate any transient bedding-plane foliation. A later D_2 event then affected the rock, folding S_1 into a spaced crenulation cleavage (sub-horizontal in Figure 32), which we can call S_2. Metamorphism may or may not accompany D_2 and the folding of S_1. If it does, new M_2 mica growth will develop parallel to S_2.

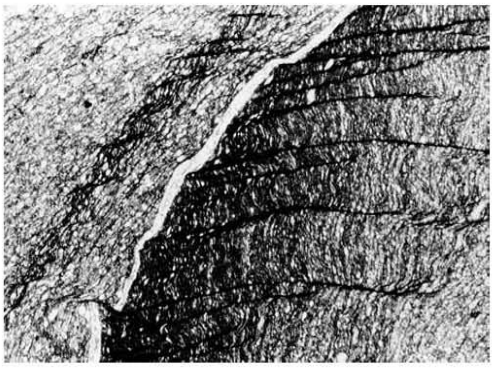

FIGURE 32 Pelitic schist with three s-surfaces. S_0 is the compositional layering (bedding) evident as the quartz-rich (left) half and mica-rich (right) half. S_1 (subvertical) is a continuous slaty cleavage. S_2 (subhorizontal) is a later crenulation cleavage. Field width ~4 mm. From Passchier and Trouw (2005). Copyright © with permission from Springer-Verlag.

S_1 is most obvious in the microlithons between the spaced S_2 cleavages in the micaceous layer in Figure 32 because micas are platy and define cleavages well. S_1 and S_2 are also visible in the slightly more mica-rich layer within the sandy bed. Crenulation cleavages become more distinctive when the fold limbs get tighter and asymmetrical (Figure 25) and quartz grains are removed from the limbs by solution transfer (Figure 24). If D_2 is accompanied by a metamorphic event (M_2), growth of new micas along the steep limbs or axial planes will further define S_2 (Figures 24 and 25). If D_2 is intense or recrystallization accompanying M_2 is sufficiently thorough, S_1 textures may become overprinted to the extent that they are no longer visible. In Figure 32, M_2 metamorphism did accompany S_2 development because quartz has been removed from the S_2 cleavages, leaving a micaceous and opaque graphite residue (horizontal black bands).

Although these observations may appear to be tiny details seen at the microscopic scale, let me remind you that large-scale and dramatic events, such as the collision of India and Asia, may produce some awesome geologic and topographic features, but erosion will one day remove the grandeur of such spectacles. All that will remain is the exposed deformed metamorphic rocks, which hold the only lasting clues to those ancient events. Structural geologists and metamorphic petrologists unravel the history of those events by the types of observations that I have just described. The Taconic and Acadian orogenies in New England, for example, produced some mountains that once probably looked much like the Himalayas. Today we might see an Acadian S_2 crenulation cleavage overprint a Taconic S_1 cleavage, that may be the only local record of that history in some places.

In order to interpret the metamorphic and deformational history of a rock, it is useful to be able to distinguish metamorphic mineral growth from deformational phases. Deformation and metamorphism generally occur in unison as dynamic recrystallization in orogenic metamorphism, but this is not always the case. Metamorphic mineral growth can be constrained on the basis of the timing of growth with respect to deformation. Mineral growth may thus be characterized as **pre-kinematic**, **syn-kinematic**, or **post-kinematic**. Many investigators use the term "tectonic" in place of "kinematic," but this has genetic implications (however broad), so I prefer the less encumbered term that simply indicates motion. A fourth category of porphyroblasts, **inter-kinematic**, implying mineral growth that is post-kinematic to one deformational event and pre-kinematic to the next, is less commonly used, but the term may be useful when the distinction is clear. It may be difficult to clearly assign the growth of a mineral to one of the categories. For example, minerals that define a good crystallization schistosity (as in Figure 23) may have

grown syn-kinematically, but growth may have outlasted deformation and continued post-kinematically.

Porphyroblasts are among the most useful tools for interpreting metamorphic-deformational histories for several reasons. First, porphyroblasts, being larger than the matrix around them, are mechanically more resistant to deformation, and can thus become porphyroclasts during later shearing, and be used as sense-of-shear indicators. Second, porphyroblasts may envelop and include some finer grains as they grow, thus becoming **poikiloblasts**. The nature and pattern of the inclusions may be very useful in interpreting deformation-mineral growth histories.

If the matrix was foliated before poikiloblast growth, the inclusions within the porphyroblast may record that earlier foliation as an **internal *S*** (S_i), as seen in two of the bands in Figure 33. Note that a foliated S_i within a poikiloblast cannot be formed by deformation of a poikiloblast with random inclusions (unless the poikiloblast is unusually weak and severely deformed). Internal *S* foliations must have been developed *prior to* porphyroblast growth and then enveloped by the growing porphyroblast. If a foliation becomes partially or completely obliterated in a rock matrix due to strong later deformation (± metamorphism), the S_i in the poikiloblast may be the only surviving record of the earlier *S*-forming event.

A porphyroblast may also include a mineral that becomes a reactant in a later metamorphic reaction. Because diffusion within a crystal is slow, the porphyroblast may protect the inclusions, which may then be the only remnant of that mineral if it is completely consumed in the matrix. Such protected inclusions are called **armored relics**. If the inclusion is an important index mineral or an indicator of metamorphic grade, it is particularly valuable in the interpretation of the history of the rock.

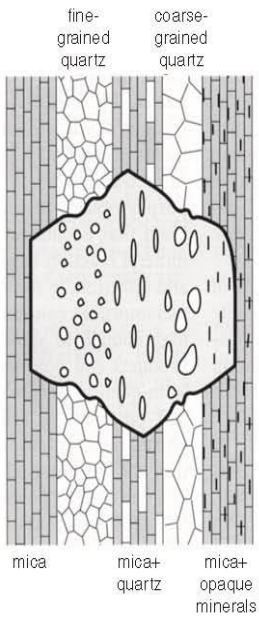

FIGURE 33 Illustration of an Al_2SiO_5 poikiloblast that consumes more muscovite than quartz, thus inheriting quartz (and opaque) inclusions. The nature of the quartz inclusions can be related directly to individual bedding substructures. Note that some quartz is consumed by the reaction, and that quartz grains are invariably rounded. From Passchier and Trouw (2005). Copyright © with permission from Springer-Verlag.

A careful petrographer may be able to infer several useful clues about the history of metamorphism, deformation, and growth of metamorphic minerals by observing inclusions and their orientation with respect to the foliation outside a porphyroblast (Zwart, 1960, 1962). When S_i is compared to an external foliation, the external one is typically referred to as the **external *S***, or S_e, regardless of whether S_e is S_1 or S_2, etc.

As described earlier, porphyroblasts grow larger than matrix minerals because their nucleation rate is much slower than their growth rate. Nucleation from a melt or a glass is considered *homogeneous* because the matrix in which they grow is uniform. Nucleation in metamorphic rocks is *heterogeneous*, however, because there is usually a variety of preexisting surfaces on which a new mineral may nucleate. Various crystal surfaces in different lattice orientations, different mineral-pair grain boundaries, crack and fracture surfaces, fluids, impurities, irregularities and deformed areas all make for a plethora of possible nucleation sites in rocks. Some investigators use this variety to argue that nucleation must be easy, and that porphyroblasts must then result from rapid growth rates for certain minerals (perhaps the introduction of some critical component in a fluid). But there are clearly fewer nuclei formed, so others argue that a variety of nucleation sites does not guarantee that all minerals will nucleate equally easily, and that porphyroblasts require either larger initial clusters to be stable or very special sites. One thing is clear: phyroblasts involve more extensive growth on fewer nuclei than the other minerals in a rock. Common porphyroblast-forming minerals are garnet, staurolite, andalusite, kyanite, cordierite, and albite, but a number of other minerals may form porphyroblasts under favorable circumstances.

As I said above, it may not always be possible to determine unequivocally the relationship between metamorphic mineral growth and deformation, but the following is intended to be a useful guide.

Pre-kinematic crystals (Figure 34), when clearly recognizable, show the usual characteristics of minerals affected by later deformation, most of which are described above for high-strain rocks. These include undulose extinction, cracked and broken crystals, deformation bands and twins, kink bands, pressure shadows, porphyroclasts with mortar texture or sheared mantles, etc. **Pressure shadows** (Figure 34c) occur when solution transfer dissolves a mineral (usually a matrix mineral) from high-stress areas (generally in the σ_1 direction) and re-precipitates it in low-stress areas adjacent to a porphyroblast. In addition, the external foliation may be **wrapped**, or compressed about a pre-kinematic porphyroblast, a result of flattening in the matrix. S_i is of little use in determining the relationship between a porphyroblast and *later* deformational events.

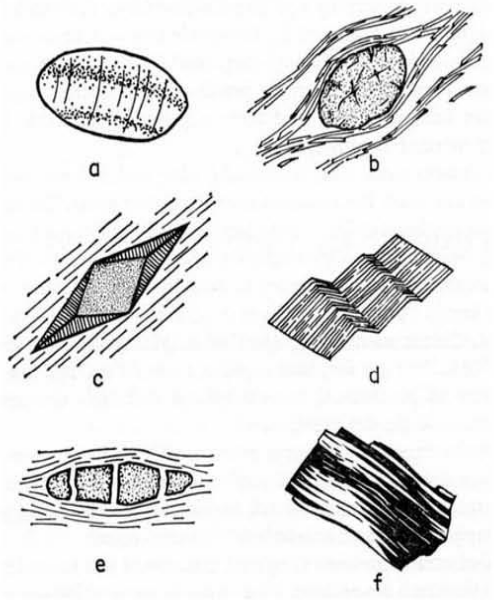

FIGURE 34 Typical textures of pre-kinematic crystals. (a) Bent crystal with undulose extinction. (b) Foliation wrapped around a porphyroblast. (c) Pressure shadow or fringe. (d) Kink bands or folds. (e) Fragmented and stretched crystals (microboudinage). (f) Deformation twins. From Spry (1969).

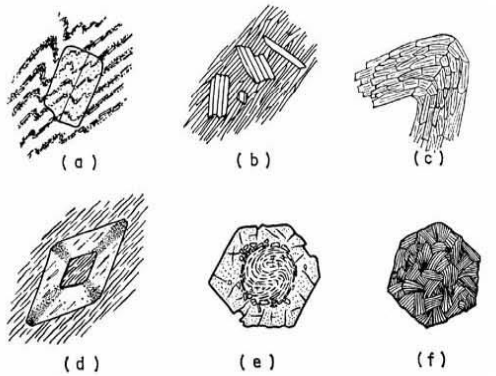

FIGURE 35 Typical textures of post-kinematic crystals. (a) Helicitic folds in S_i. (b) Randomly oriented elongate crystals. (c) Polygonal arc of straight crystal segments in a fold. (d) Chiastolite with central S_i concordant with S_e. (e) Late, inclusion-free rim on a poikiloblast. The rim *may* be post-kinematic. (f) Random aggregate of grains of one mineral pseudomorphing a single crystal of another (chlorite after garnet). The chlorite is post-kinematic. From Spry (1969).

Post-kinematic crystallization either outlasted deformation or occurred in a distinct later thermal or contact event. When clearly distinguishable, both the previous deformation and the later mineral growth or recrystallization must be apparent. Post-kinematic growth results in unstrained crystals. In many cases, the crystals are randomly oriented and cut across an earlier foliation (Figure 35b), although mimetic growth may cause a large proportion of later crystals to grow parallel to the foliation anyway.

Pseudomorphs (Figure 35f), particularly those in which a crystal is replaced by an aggregate of random smaller crystals, suggest that the replacement was post-kinematic. Bent crystals may polygonize during later static growth to smaller unstrained crystals. A dramatic example of this is the **polygonal arc** (Figure 35c), in which folded elongate minerals polygonize to an arcuate pattern consisting of smaller straight crystals. If post-kinematic recrystallization is extensive, a granoblastic or decussate texture may be developed, and an earlier foliation may be difficult or impossible to discern. When an internal S is visible in poikiloblasts, the pattern of S_i may be useful. For example, **helicitic folds** (Figure 35a) mean that S_i is folded. Because a poikiloblast with a straight S_i cannot be deformed so that the S_i becomes folded, helicitic folds indicate that the porphyroblast grew after both S_1 and S_2 (the axial surfaces of the folds) had formed. Helicitic folds are thus an indicator of post-kinematic porphyroblast growth.

A poikiloblast with a straight S_i that is parallel to, and continuous with, S_e (Figure 35d, Figure 37-3a) is also *probably* post-kinematic because it is most easily explained by the growth of a porphyroblast in a static situation over an existing schistosity. A later deformation may rotate an earlier porphyroblast or transpose S_e. Thus if S_i is not parallel to, or continuous with, S_e the porphyroblast is either pre-kinematic to D_2, or syn-kinematic and deformation outlasted porphyroblast growth. It may be impossible to distinguish between these two possibilities.

Syn-kinematic mineral growth is probably the most common type in orogenic metamorphism because metamorphism and deformation are believed to occur generally in unison. It is also the most difficult to demonstrate unequivocally. A continuous schistosity, as illustrated in Figure 23, was probably generated by a process of dynamic (syn-kinematic) recrystallization. Aligned grains that are a mixture of bent crystals with undulose extinction and straight recrystallized grains support this conclusion more strongly, although they could also be a less likely combination of pre-kinematic and post-kinematic crystallization. It is probable, but largely a matter of faith, then, that syntectonic crystallization occurs during the development of a schistosity.

Misch (1969) described one clear indicator of definitively syn-kinematic mineral growth. Figure 36 is an example of "syn-crystallization micro-boudinage." Although boudinage of individual crystals has been described from several localities, it is usually an indication of pre-kinematic crystals that have been stretched after their growth. In the case described by Misch, however, the crystals are clearly zoned, as seen in thin section by a gradation from colorless amphibole cores to blue rims. The concentric pattern of zoning occurs *between* the separated tablets, as well as around them, reflecting growth added *during* separation.

It is also widely believed that syn-kinematic porphyroblasts are the most common type of porphyroblast, probably due to the catalyzing effect that deformation has on nucleation, reaction, and diffusion rates (Bell, 1981; Bell

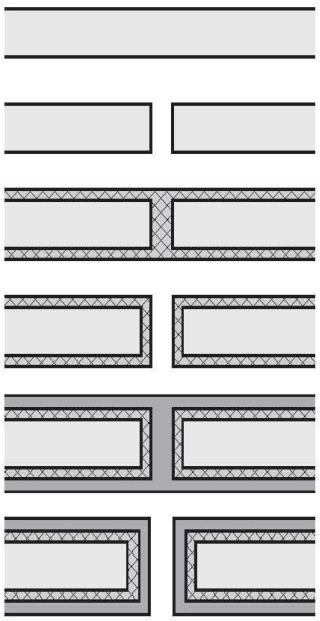

FIGURE 36 Syn-crystallization micro-boudinage. Syn-kinematic crystal growth can be demonstrated by the color zoning that grows and progressively fills the gap between the separating fragments. After Misch (1969). Reprinted by permission of the *American Journal of Science*.

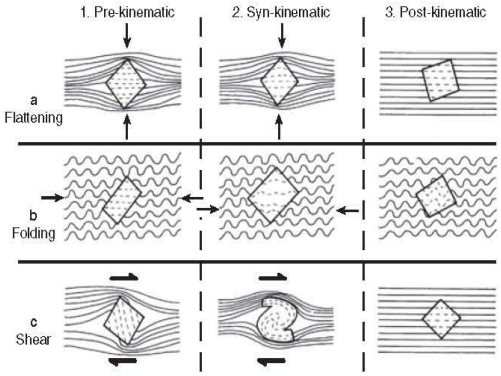

FIGURE 37 S_i characteristics of clearly pre-, syn-, and post-kinematic crystals (columns 1–3: left-to-right) as proposed by Zwart. **(a)** Top row: flattening. **(b)** Middle row: folding. **(c)** Bottom row: shear/rotation. The pre-, syn-, and post- prefixes refer to the flattening, folding, or shear event, not the earlier development of S_1. After Zwart (1962).

and Hayward, 1991; Baxter and DePaolo, 2004), but proof of syn-kinematic growth is rare. In certain instances, however, the pattern of S_i inclusions in a porphyroblast may provide unequivocal evidence for syn-kinematic porphyroblast growth (Zwart, 1960, 1962). Figure 37 illustrates porphyroblast growth incorporating an S_i, associated with (a) flattening, (b) folding, and (c) shear. Let's begin with row (a)—*flattening*. Imagine a deformation (D_1) that produced a foliation (S_1), followed by *post-kinematic* poikiloblast growth that then incorporated the *uniform* S_1. This would be the case for column 3 (right side) of row (a), or 3(a), where the poikiloblast must have grown entirely after the foliation was developed. Next imagine that S_1 becomes flattened. In box 1(a) the poikiloblast grew after S_1 but is *pre-kinematic* to flattening, during which the foliation was compressed around the poikiloblast. This may be a good example of *inter-kinematic* porphyroblast growth, but the illustration is attempting to address the flattening, which the bending around the porphyroblast suggests was produced by a second D_2 event. The S_i pattern in the center figure of row (a), box 2(a) is (finally) an example of demonstrable syn-kinematic porphyroblast growth because it shows a systematic variation in the spacing of S_i from core to rim. The wider spacing of S_i at the core indicates that the poikiloblast grew initially over a less flattened S_1, and successive layers of poikiloblast growth incorporated a progressively more closely spaced foliation that was progressively flattened as the poikiloblast grew. The poikiloblast is thus demonstrably syn-kinematic to flattening. The foliation and the flattening in this case may reflect a single D_1 event.

Row (b) of Figure 37 illustrates a similar scenario, in which S_1 is *folded* and the folds in the center *syn-kinematic* example become progressively more intensely folded as the porphyroblast grows and incorporates them. 1(b) illustrates poikiloblast growth following D_1-S_1, but *pre-kinematic* to folding. Poikiloblast growth in 3(b) is entirely *post-kinematic* to both S_1 development and folding.

The bottom row in Figure 37 corresponds to *shear*. I'm sure you can now interpret 1(c) and 3(c) as poikiloblast growth that is pre-shear and post-shear. 2(c) is *syn-kinematic* and shows a **spiral** pattern of the S_i inclusions that is not found in the matrix foliation. The traditional interpretation of this spiral pattern is that the porphyroblast rotated as it grew (Figure 38), progressively incorporating the external foliation, like rolling a snowball. This spiral S_i texture is particularly common in garnets. Some call the spiral texture **rotated**, or, if the rotation is extensive, **snowball** (Figure 39). Note that the spiral creates a fold pattern, but the spiral is a special case of a fold and has rotational symmetry. It is important to distinguish this spiral pattern as separate from helicitic folds (which indicate post-kinematic poikiloblast growth).

In all three situations in the left column of Figure 37, pre-kinematic porphyroblasts have a straight, parallel S_i (= S_1), and the S_e has either rotated, wrapped, or folded after porphyroblast growth, presumably during a separate later deformational event (D_2). Barker (1990) argued, however, that porphyroblasts can grow relatively quickly, and may envelop a straight S_i during the early stages of a deformation event and still be rotated, flattened, or folded during the same event. Syn-kinematic porphyroblasts (center column in Figure 37) show progressively spiraled, flattened, or folded S_i. Post-kinematic porphyroblasts (right column in Figure 37) overgrow the sheared, compressed, or folded S_1 without a discontinuity between S_i and S_e. When S_i is not continuous with S_e it means that either a separate deformation affected it, or that porphyroblast growth ceased before deformation did, and a single deformation created the S_i and then the discontinuity.

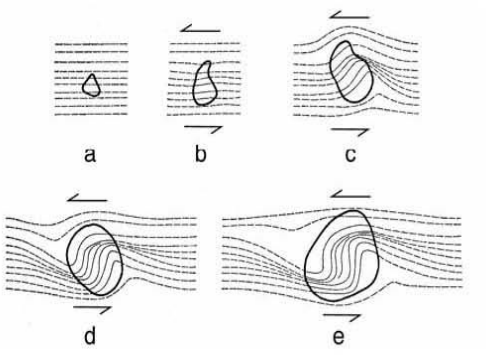

FIGURE 38 Traditional interpretation of spiral S_i train in which a porphyroblast is rotated by shear as it grows. From Spry (1969).

The traditional interpretation of rotated porphyroblasts has been challenged by Ramsay (1962), Bell (1985), and others. Ramsay (1962) first suggested that rigid porphyroblasts (at least equidimensional ones such as garnet) may remain spatially fixed during deformation, and that the *foliation is rotated* about the porphyroblast instead. Some works (Fyson, 1975, 1980; Johnson, 1990; de Wit, 1976; Bell et al., 1992) have demonstrated consistent porphyroblast orientations on a regional scale, or even on opposite sides of folds (where the sense of shear should be opposite), which support the notion that the foliation was rotated, and not the porphyroblast. It may be hard to imagine rotation of a regional foliation more than 90° or so, and extreme examples of spiral inclusion trails (Figure 39) may support rotated porphyroblasts, but for the much more common occurrence of $<90°$ rotations, it is still controversial as to what mechanism occurred. There is little disagreement that elongate porphyroblasts may be rotated, and the controversy is over equidimensional ones, such as garnets. For discussions of this controversy, see Bell et al. (1992); Passchier et al. (1992); Williams and Jiang (1999), Vernon (2004), and Passchier and Trouw (2005).

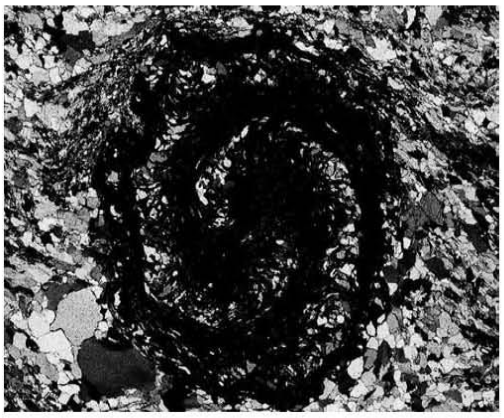

FIGURE 39 "Snowball garnet" with highly rotated spiral S_i. Porphyroblast is ~5 mm in diameter. From Yardley et al. (1990). Copyright © reprinted by permission of John Wiley & Sons, Inc.

Why all the worry if there is agreement that the spiral represents syn-kinematic growth? Note in Figure 38 that the sense of shear in the rotating porphyroblast is *sinistral* (anticlockwise). If, on the other hand, the external foliation is rotated and the porphyroblast remains stationary, the same pattern would require *dextral* shear. Thus the shear sense that we deduce depends on our interpretation of what rotates. Until this controversy is resolved, it would be wise to avoid depending upon spiral inclusion trails alone to determine sense of shear. Similarly, mechanism-biased terms, such as *snowball* and *rotated* porphyroblasts, are best avoided in favor of the simple geometric term *spiral*.

Bell (1985) and Bell et al. (1986) suggested that deformation in a rock body experiencing shear is partitioned unequally as a result of primary or secondary mechanical inhomogeneities. They proposed that high-shear domains (S_2 in this situation, and they are white in Figure 40) are separated from lozenge-shaped zones of little or no strain (dark shaded) by transitional zones of mostly flattening or shortening (light shaded), depending on the style of deformation. As mentioned previously, phyllosilicates can accommodate shear better than most other minerals. High shear, they proposed, causes the other minerals to dissolve (a form of solution transfer) and migrate to low-shear areas where, they believe, porphyroblasts tend to form. This results in *metamorphic differentiation* into mica-rich and mica-poor/porphyroblast-rich domains (P and Q, as described previously).

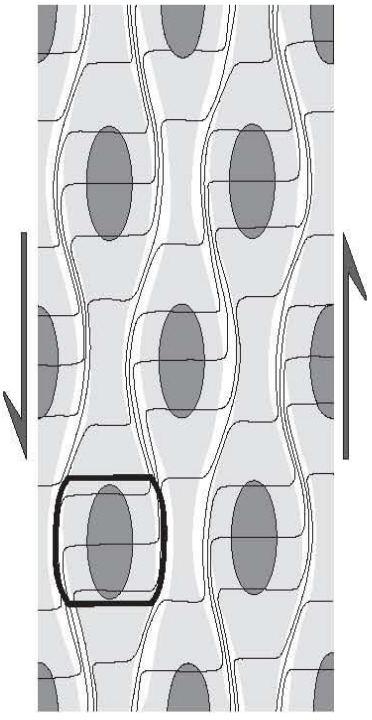

FIGURE 40 Non-uniform distribution of shear strain as proposed by Bell et al. (1986). Blank areas represent high shear strain and dark areas are low strain. Lines represent initially horizontal inert markers (S_1).

Note that a porphyroblast that grows in a low-shear area but eventually extends into the marginal area of transition, such as the one outlined in Figure 40, can develop an inclusion trail that is straight in the center (from an earlier S_1) and spiraled toward the rims. This is a common shape for S_i in poikiloblasts, which Bell et al. (1986, 1992) and Bell and Johnson (1989) interpreted to be *unrotated* because the porphyroblast simply grows over a folded foliation. The straight to spiraled S_i in the porphyroblast was attributed above to pre-kinematic (to S_2) core growth, followed by a syn-kinematic rim, but the porphyroblast in question here is entirely late syn-kinematic to S_2 if this interpretation is correct. Bell et al. (1992) also proposed that the sheared zones (white areas in Figure 40) may expand with time into the low-shear areas and the porphyroblasts, causing porphyroblasts to dissolve and the S_i to become truncated. They suggested that this common pattern of straight S_i in porphyroblast cores with spiraled rims occurs because porphyroblasts do not tend to grow during the first deformation (D_1) of pelitic sediments (the one that produced the initial S_1 in Figure 40) because poor lithification results in more evenly distributed strain and more compression as the sediments lose pore fluids. Only during D_2, when the rock is more competent, does the above scenario take place and S_1 is found in the porphyroblast cores.

The deformational history of porphyroblasts without an internal S is difficult to interpret with confidence. Undeflected S_e at porphyroblast margins is traditionally taken to indicate post-kinematic porphyroblast growth, which does not disturb a preexisting foliation, but deflection of S_e is less certain. Ferguson and Harte (1975) suggested that deformed and deflected S_e around a porphyroblast could reflect pre-, syn-, or post-kinematic porphyroblast growth and warned against using any interpretation of S_e at porphyroblast margins when S_i is missing. When pressure shadows are present, or the external foliation is deflected, the porphyroblast is probably pre-kinematic, but there could be several kinematic events.

A long-standing controversy has focused on foliations that wrap around porphyroblasts (Figure 34b). Some investigators (Ramberg, 1947; Misch, 1971, 1972a, b) have argued that growing crystals exert a "force of crystallization" that can physically bow out an earlier foliation, similar to ice-wedging during weathering. Others (Rast, 1965; Spry, 1969, 1972; Shelley, 1972) have argued that metamorphic porphyroblasts grow by infiltration along grain boundaries and replacement of preexisting minerals and cannot exert enough force to displace neighboring grains. Yet others (Yardley, 1974; Ferguson, 1980) argued that the foliation may migrate and appear bowed by pressure-solution associated with a growing porphyroblast. I think most petrologists lean toward the notion that it is simpler for a foliation to deform around an existing porphyroblast than for the porphyroblast to affect the foliation. In several situations, this has been amply demonstrated to be the case, whereas the opposite is less certain. Wrapping of foliation about a porphyroblast, particularly if it is well developed or associated with a discontinuity between S_i and S_e is thus generally taken to indicate that the foliation has been compressed around the porphyroblast. No warranty, however, comes with this claim.

Passchier and Trouw (2005) noted two further complications in interpreting mineral growth–deformation relationships in metamorphic rocks. First, it may be possible for two deformation phases to be of similar orientation and thus indistinguishable texturally or structurally. Second, the opposite may also be true: one deformation phase may produce both a foliation and a folding of that foliation (Figure 41). In this case both S_1 and S_2 are produced by a single consistent and progressive event, even though S_2 appears to overprint S_1. Such folded foliations are observed in several shear zones, in which a single shearing event is all but assured. I doubt that the development of a penetrative crenulation cleavage can be developed over a broad area in this fashion, however, and suspect that single-stage folded foliations develop more locally, initiated perhaps by inhomogeneities. Even in the shear zone examples, the secondary folds typically occur as local folds that do not develop in all layers. Although we must understand that our interpretations may miss some historical event, we can only assume the simplest and most straightforward explanations of the textures that we observe. We thus interpret foliations to represent a single phase of deformation, and folds to represent a separate phase for the structures that they affect. Only when intensive and well-distributed

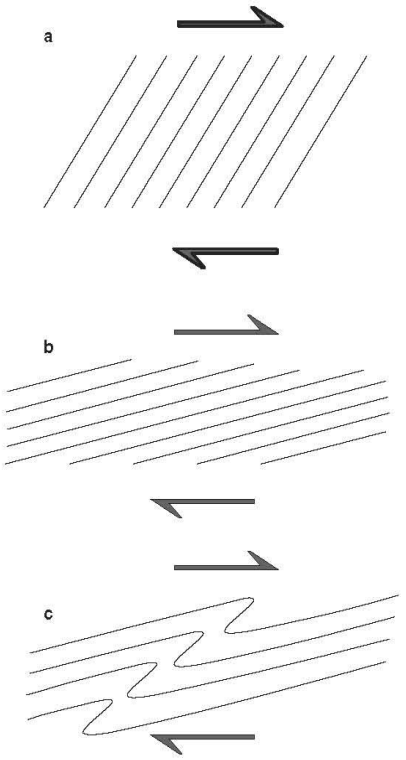

FIGURE 41 **(a–b)** Initial shear strain causes transposition of foliation. **(c)** Continued strain during the same phase causes folding of the foliation.

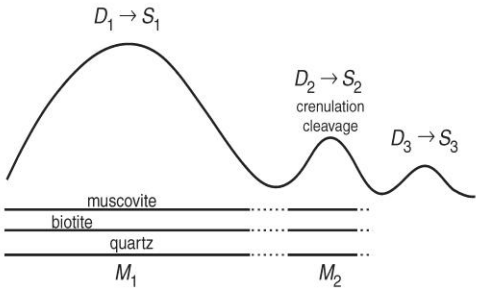

FIGURE 43 Graphical analysis of the relationships between deformation (*D*), metamorphism (*M*), mineral growth, and textures in the rock illustrated in Figure 42.

possible to say with certainty whether the matrix rotated 170° dextrally (clockwise) or the garnet rotated 170° sinistrally (anticlockwise). The slight asymmetry in the upper quartz-rich layer, stair-stepping upward to the left, vaguely suggests sinistral rotation (Figure 19), but unless other shear-sense indicators are found elsewhere in the rock, any conclusion based strictly on the S_i in garnet should be considered provisional. Note also that the thickness of the quartz-rich layers is greater at the garnets. The simplest explanation for this effect is that the layering was compressed about the garnets by the same deformation responsible for the rotation.

Note also that quartz has a well-developed granoblastic polygonal texture in the quartz-rich layers but is elongated in the mica-rich layers. The good polygonal texture suggests that crystallization outlasted deformation, which is also reflected in the generally straight micas and continuity between S_i and S_e of the garnets. The elongation of quartz in the micaceous layers is probably controlled by the micas (as discussed above: Figure 11). The quartz inclusions in the garnet are also elongated, and these inclusions may have been part of originally quartz-rich layers. If so, this suggests that perhaps the quartz crystals were elongated in both the mica-rich and mica-poor of layers when the garnet was growing, and the granoblastic texture in the quartz-rich layers occurred later. Alternatively, perhaps the garnet began to grow prior to metamorphic differentiation and completely replaced the micas (scavenging the Al, and perhaps Fe and Mg) that controlled quartz elongation. Metamorphic differentiation then separated the "Q-rich" and "M-rich" layers at a later point, perhaps due to more advanced shear or at the metamorphic peak temperature.

A final factor is the number of deformational phases involved in Figure 44. Clearly, there was an S_1 prior to garnet growth. The simplest explanation for the growth of the garnet and the rotation that created the spiraling is that the garnet grew late during S_1, and the same deformation caused the rotation and the compression of the layering. This is consistent with the notion that garnet occurs at a higher metamorphic grade than quartz recrystallization and muscovite + biotite growth. A graphical interpretation would then look like Figure 45. Had S_i been discontinuous with $(S_i \neq S_e)$ then the deformation curve would have extended past the lines representing crystallization. Although a second minor deformation event cannot be ruled out, a single event is a simpler explanation.

As a third example, consider Figure 46. In this case, there is a distinct S_1 in muscovite that has been folded to develop a good set of S_2 axial planes. Large andalusite porphyroblasts then formed in a random orientation with good helicitic folds in S_i. Andalusite growth is interpreted as the result of a later contact metamorphic overprint (presumably supported by field relationships). Note that the S_i pattern could almost be a spiral, but the fact that $S_i = S_e$ in identical external folds shows that the inclusion texture must be helcitic. The well-developed polygonal arcs could indicate that muscovite crystallization outlasted D_2 deformation or that the contact event caused muscovite recrystallization that was largely mimetic to the preexisting folded muscovite. Figure 47 is a graphical interpretation. Whether D_1 and D_2 were deformation phases associated with a single M_1 or two metamorphic events is purely speculative.

It is imperative to remember that this type of analysis can contribute valuable data to a structural synthesis of an area, but to be done properly it must be integrated with good structural field work. A simple straight S_1 in thin section, for example, may be parallel to the axial planes of folds too large to be seen in a thin section. Note also that polydeformed and polymetamorphosed rocks are relatively common, and

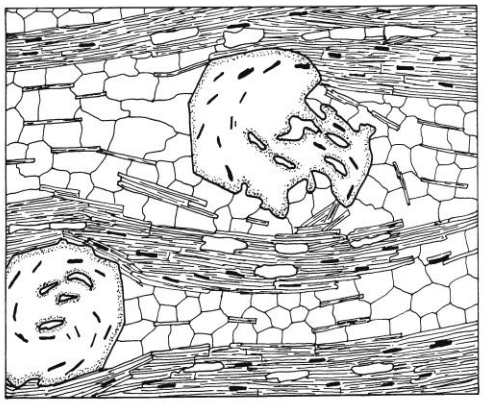

FIGURE 44 Composite sketch of some common textures in Pikikiruna Schist, New Zealand. Garnet diameter is ~1.5 mm From Shelley (1993). Copyright © by permission Kluwer Academic Publishers.

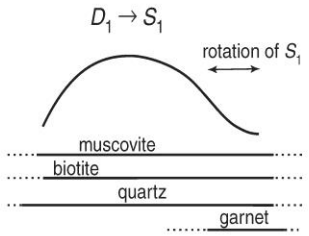

FIGURE 45 Graphical analysis of the relationships between deformation (*D*), metamorphism (*M*), mineral growth, and textures in the rock illustrated in Figure 44.

FIGURE 46 Textures in a hypothetical andalusite porphyryoblast–mica schist. After Bard (1986). Copyright © by permission Kluwer Academic Publishers.

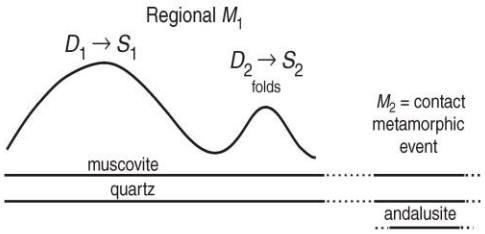

FIGURE 47 Graphical analysis of the relationships between deformation (*D*), metamorphism (*M*), mineral growth, and textures in the rock illustrated in Figure 46.

that the classification of crystallization into pre-, syn-, and post-kinematic types may often be oversimplified. In polymetamorphic rocks, one should be clear as to which event or textural element a prefix is related (e.g., pre-kinematic to S_2).

As a more complex example of a polymetamorphic rock, consider Figure 48, which shows three stages in Spry's (1969) interpretation of the final rock texture (Figure 28c). The matrix minerals are muscovite and quartz, whereas the porphyroblasts are garnet (G) and albite (Ab). Notice how S_2 mica growth has become sufficiently pronounced to obliterate most of the evidence for S_1, which is only discernable in the microlithons and S_i of the poikiloblasts. S_0 is only preserved as an S_i as well.

As a final note on orogenic metamorphism and deformation in an orogenic belt, consider Figure 49, a hypothetical scenario for the development of an orogen. In this scenario, an island arc terrane develops offshore from a continental mass. At stage I, deformation (D_1) occurs in the forearc subduction complex (A) associated with the arc (B). In detail, this deformation typically migrates away from the volcanic arc and toward the trench (to the left in the figure). Thus D_1 deformation is not concurrent at all points within A and does not occur within B or C at all. By stage II, D_2 deformation overprints D_1 within A in the form of subhorizontal folding and back-thrusting, which develops as the right side of the forearc package is pushed against the resistant igneous arc crust. D_1 is still occurring on the left side of A at the same time. Subduction is initiated at C in stage II, and D_1 deformation (as locally defined) begins here (also migrating left toward the trench). Subduction-related igneous activity develops behind C as the arc matures. The same development of D_2 deformation against the continental crust may develop in area C as occurred during stage I in area A. In stage III, the offshore terrane is accreted to the continent, thereby creating a **suture zone**, and terminating subduction in area C. Because of the intensity of the collision, local D_1 deformation may penetrate the resistant sialic crust of both the arc and the continent. Within area B, the initial D_1–S_1 foliation has been overprinted by S_2 folds during stage III, perhaps as parts of a single event (as in Figure 41). Renewed (D_2) thrusting cuts the outermost foliation in the outer portions of the wedge in area C. D_2 deformation may also be associated with a later phase of collapse of the orogen.

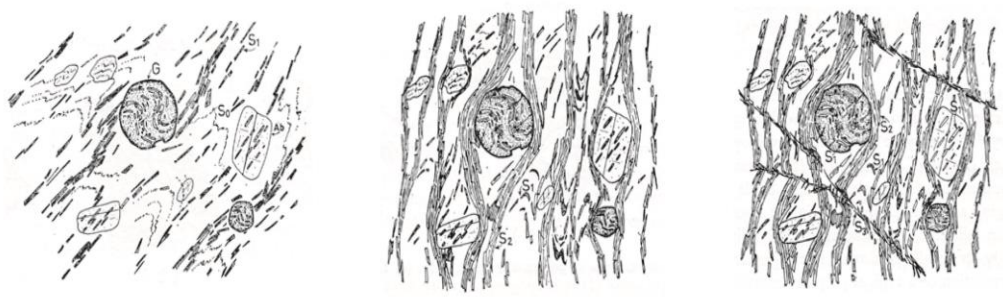

FIGURE 48 Interpreted sequential development of a polymetamorphic rock. From Spry (1969).

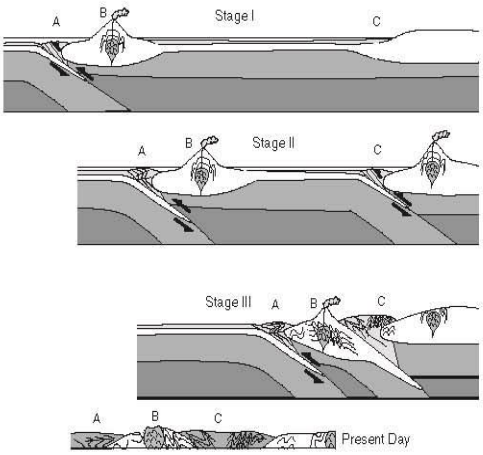

FIGURE 49 Hypothetical development of an orogenic belt involving development and eventual accretion of a volcanic island arc terrane. See the text for discussion. After Passchier and Trouw (2005). Copyright © with permission from Springer-Verlag.

The scenario depicted above is hypothetical but consistent with the types of processes that we believe occur during the plate tectonic development of an orogenic belt. Note that deformation is neither of the same style nor is any phase simultaneous throughout the resulting belt. D_1, at one point, may be a different deformation than D_1 elsewhere, and may occur at the same time as D_2 or D_3 in another part of the orogen. Most mountain belts are an amalgamation of assembled terranes, each with its own unique history. Similarly, deformation may change style in a single locality, and deformation of a single style may migrate, so as not to be synchronous, even in adjacent rock packages. One can only unravel the history of such a complex orogen by careful integration of petrographic, structural, isotopic, sedimentary, and igneous data collected throughout the orogen.

Analysis of deformational and metamorphic histories based on textures and structural data is a difficult task and readily subject to oversimplification and interpretive errors. This has been only a cursory introduction to the techniques. Students are advised to read Jamieson (1988), Passchier and Trouw (2005), and Vernon (2004) for guidance and warnings before attempting independent work. In Section 7 we will see how we can combine textures with geochronology to determine the absolute timing of some events. Among other benefits this approach may eventually solve some of the textural controversies described above.

5 CRYSTALLOGRAPHICALLY CONTROLLED INCLUSIONS

Not all inclusion patterns reflect passive envelopment of a preexisting matrix texture into a growing porphyroblast. Some patterns are controlled by the lattice or growth surfaces of the porphyroblast itself. For example, inclusions may

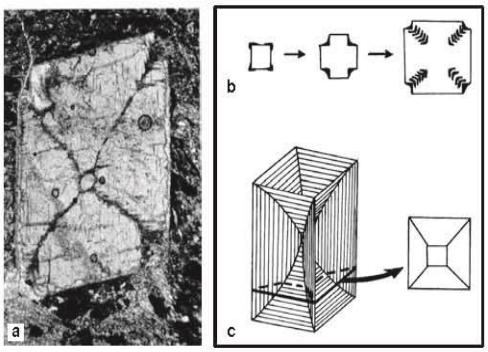

FIGURE 50 Chiastolite cross in andalusite (a) and Frondel's (1934) theory for its development (b and c). From Shelley (1993). Copyright © by permission Kluwer Academic Publishers.

adsorb preferentially onto a face or some other part of a euhedral porphyroblast. A common example is the feathery **chiastolite cross** that forms in some andalusite crystals (Figure 50). There are several theories on the origin of chiastolite, summarized well by Spry (1969) and Shelley (1993). The best explanation, in my opinion, is that proposed by Frondel (1934), who proposed that the cross forms by the selective attachment of impurities (typically graphite) at the rapidly growing corners of the andalusite. The concentration of the impurity (Figure 50) retards corner growth, forming a re-entrant, where the impurity gradually becomes incorporated by further porphyroblast growth. Repetition of the growth-retardation-growth scenario results in the feather-like appearance along four radiating arms. Similar patterns in other minerals, such as garnet, have been reported, but are much less common. Another crystallographically controlled inclusion pattern is **sector zoning**, in which inclusions are preferentially incorporated on some faces of a growing crystal (typically the faster-growing faces). If this occurs only on one pair of growing faces it produces an **hourglass** pattern (Figure 51), observed in some staurolite and chloritoid crystals.

These oriented inclusion patterns should be distinguished from **exsolution** of a dissolved phase, such as perthite, etc., which can also produce crystallographically oriented lamellae of one mineral in another. The crystallographically controlled needles of rutile in some biotite or hornblende crystals, for example, are exsolution phenomena, and are not oriented because of their envelopment by the host mineral.

6 REPLACEMENT TEXTURES AND REACTION RIMS

Replacement and reaction textures typically develop when reactions do not run to completion. Although it may seem more tidy to have all things run to completion, most petrologists are delighted to find replacement/reaction textures because they indicate the nature, direction, and progress of a reaction. These textures may provide clues to the nature of the protolith or the history of rocks sampled.

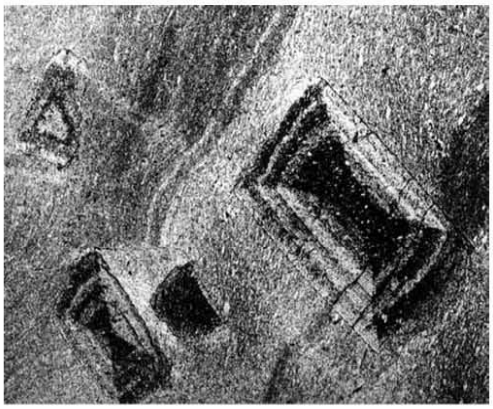

FIGURE 51 Euhedral chloritoid porphyroblasts in a fine-grained schist with hourglass zoning and rhythmic layer zoning, both of which are due to differing concentrations of inclusions. The hourglass zoning is crystallographically controlled, whereas the layer zoning must be related to varying conditions of growth. Field width ~8 mm. From Passchier and Trouw (2005). Copyright © with permission from Springer-Verlag.

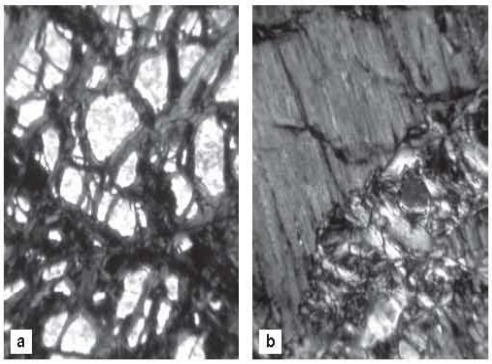

FIGURE 52 (a) Mesh texture in which serpentine (dark) replaces a single olivine crystal (light) along irregular cracks. (b) Serpentine pseudomorphs orthopyroxene to form bastite in the upper portion of the photograph, giving way to mesh olivine below. Field of view ca. 0.1 mm. Fidalgo serpentinite, Washington.

Replacement occurs when the reaction products replace a reacting mineral. Some degree of retrograde metamorphism typically occurs during the cooling of plutons because the rocks are maintained at metamorphic temperatures for extended periods. A wide range of retrograde reactions are possible in both igneous and metamorphic rocks. Perhaps the most common are hydration reactions, such as those that produce chlorite rims on mafic minerals. Retrograde metamorphism is less likely than prograde to reach equilibrium, commonly resulting in replacement textures.

In many replacement reactions, a **pseudomorph** may develop, in which the reaction products retain the shape of the original mineral. Even if the pseudomorphing reaction runs to completion, the texture might still be used to interpret the reaction if the original mineral can be recognized by the shape of the pseudomorph. Some reactions produce intimate, typically wormy-looking, intergrowths of two or more minerals, a texture called **symplectite**. Pseudomorphs may thus be either monomineralic or a symplectitic intergrowth. Some replacement styles can be specific to certain mineral types. For example, in serpentinitized ultramafics the original olivines are typically replaced by serpentine along cracks in a net-vein-like **mesh** pattern (Figure 52a). Small relict olivine islands may remain in the network, forming an array of subgrains that all go extinct in unison, testifying to their once having been part of a larger single crystal. Orthopyroxene, if present in the same ultramafic protolith, is usually completely pseudomorphed by more uniform areas of fibrous serpentine, called **bastite** (Figure 52b).

Reaction rims involve reaction between minerals where they meet at grain boundaries, resulting in the partial replacement of either or both minerals adjacent to their contact. If the reaction product forms a complete rim around a mineral it is called a **corona**. Coronas can be either monomineralic or polymineralic. Polymineralic intergrowths of small elongate grains are called **symplectitic coronas**.

Reaction rims occur when reactions did not reach completion, and are thus frozen records of reactions caused by changes in metamorphic conditions. They may reflect retrograde alteration, polymorphic transformations, diffusion of material along grain boundaries, or solid-state reactions. The latter process forms the most dramatic **coronites** (rocks with prominent corona textures), which are most common in high-grade dry rocks where slow cooling permits retrograde reactions and the lack of water keeps the reactions from running more readily to completion.

Figure 53 shows two minerals, A and B, that react to form either a new mineral C or two minerals C and D. If diffusion is limited and/or reaction time is short, the reaction product(s) may be limited to a zone at the A-B contact.

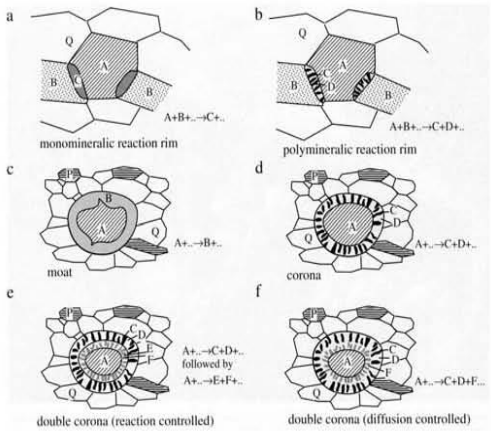

FIGURE 53 Reaction rims and coronas. From Passchier and Trouw (2005). Copyright © with permission from Springer-Verlag.

If one reactant is plentiful, the product(s) may form a continuous corona around the more limited reactant (Figure 53b). Monomineralic coronas (Figure 53c) are called **moats** by some investigators. Once a continuous rim is created between the reactants, they are separated, and the reaction consuming them can only continue by diffusion through the corona. As the corona becomes thicker the extent of diffusion must be greater, which may eventually stall the reaction, particularly in a cooling dry rock.

Coronas may be single rims (Figure 53c and d) or complex multiple concentric layers (Figure 53e and f). Double or multiple corona rims may be created as conditions continue to change to the extent that either the core mineral or the matrix mineral is no longer stable adjacent to the first corona, thereby reacting with it and forming another layer between them (Figure 53e). Alternatively, gradients in diffusing components may generate multiple rims at the same time (Figure 53f). Spectacular multiple coronites are developed between olivine and plagioclase in some deep-seated gabbros or anorthosites (Figure 54).

Corona textures can be combined with mineral stability analysis to provide detailed reconstruction of *P-T-t* histories. For example, Griffin (1971) interpreted the sequence in Figure 54 as developing in several stages during a cycle of deep burial and subsequent uplift and erosion of the Jötun Nappe. Harley et al. (1990) described Al-rich granulites that are retrogressed in stages from 1.1 GPa and 1000°C to 0.45 GPa and 750°C. The first stage of uplift involved reactions between sillimanite and garnet or orthopyroxene that produce rims of cordierite (a low-pressure mineral) on garnet (a high-pressure mineral) or orthopyroxene, and symplectites of cordierite and sapphirine replacing sillimanite. Further reaction consumed K-feldspar, pyroxene, and sapphirine to produce biotite, and later still biotite reacted with plagioclase and quartz to develop symplectitic rims of second-generation orthopyroxene and cordierite. Such detailed reconstructions are possible because the reactions are incomplete and the products occur as coronas at original grain boundaries. Coronas are common in scenarios that involve decompression. Perhaps decompression provides enough driving energy to initiate the reaction, but the reaction is still easily stalled by the diffusion required for the reactants to communicate through the rims.

7 TEXTURAL GEOCHRONOLOGY

Certain radiometric dating techniques have traditionally required mineral separation and concentration from a significant mass of rock in order to analyze the isotopic ratios of phases present in only accessory amounts. Such dates typically represented average ages from homogenized mineral concentrates. Because these minerals may consist of zones representing several growth episodes, such averaged ages may be nearly meaningless. Recent advances in analytical technology are now allowing us to extract age information from very small volumes of a single mineral as observed in thin section. This is opening up some exciting avenues of research in which the timing of individual tetonic/metamorphic events may be determined and pressure–temperature–time (*P-T-t*) paths may finally have real meaning in terms of time. But even these more specific ages can be a challenge to relate with confidence to other critical petrologic information, such as temperature, pressure, or specific orogenic and metamorphic events. The challenge is to know exactly what is being dated. I shall outline some of the critical new techniques in the present section and provide a few examples in which geochronology has been linked to specific te tonic/metamorphic events, emphasizing works relying on textures to make the link. In later

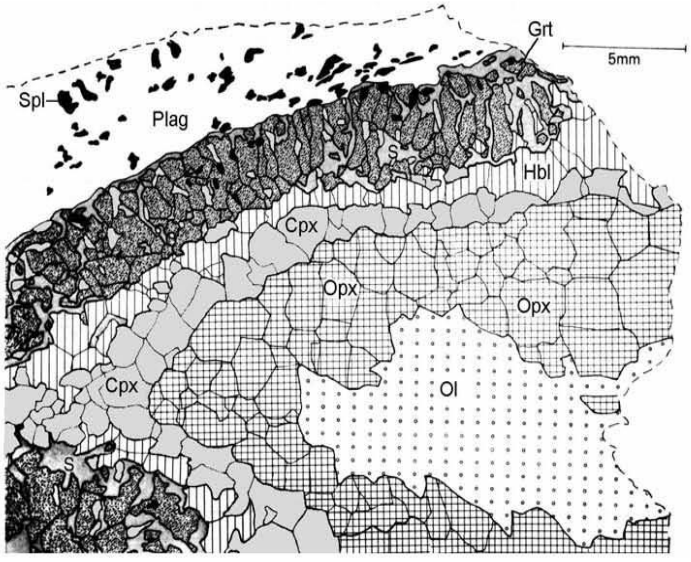

FIGURE 54 Portion of a multiple coronite developed as concentric rims due to reaction at what was initially the contact between an olivine megacryst and surrounding plagioclase in anorthosites of the upper Jötun Nappe, western Norway (from Griffin, 1971). The orthopyroxene–clinopyroxene coronas and subsequent garnet developed as the anorthosite cooled during burial and compression due to thrust stacking and nappe development. The amphibole corona developed during uplift as water became available, and later rapid uplift and decompression at relatively high temperatures resulted in the decomposition of garnet to produce a symplectitic intergrowth (S) of fine-grained orthopyroxene + plagioclase ± spinel ± clinopyroxene.

chapters we will address linking geochronology to specific reactions and/or geothermobarometry, thereby placing some time constraints on *P-T-t* paths.

7.1 Analytical Techniques and Suitable Minerals

Techniques for age determination of minute samples are rather specialized. The list below acts as an addendum to more general analytical techniques. For detailed reviews, see Parrish (1990), Harrison et al. (2002), Müller (2003), Vance et al. (2003), and Williams et al. (2007).

Thermal ionization mass spectrometry (TIMS) involves ionization of very small samples (sub-nanogram) on a filament and mass spectrometry of the ionized isotopes. The method is good for Sr and Pb isotopes of mineral separates. A finely pointed tiny diamond-tipped drill mounted on a microscope can extract (*microsample*) pieces of single mineral grains a few tens of microns across for analysis. Mineral samples can thus be observed in thin section and microsampled from specific textural situations.

Laser-ablation inductively coupled plasma mass spectrometry (LA-ICPMS). A high-power laser ablates a sample in situ, and particles are fed as a dry aerosol into an argon or helium plasma and passed into a mass spectrometer. Ultraviolet (UV) laser ablation has a spatial resolution ≤ 10 μm, so it can determine ages within zoned minerals and inclusions in porphyroblasts as they are observed microscopically.

Ion microprobe (IMP, SHRIMP), also called **secondary-ion mass spectrometry (SIMS)**, uses an ion beam (typically Cs or O) to sputter ions from a sample surface while observed in thin section and feed them into a mass spectrometer. Resolutions down to 30 μm are possible.

Electron microprobe (EMP) may already be familiar to you. Some new probes are now optimized for trace element analysis and geochronology. See the discussion of monazite below for more details. Goncalves et al. (2005) have developed a monazite age-mapping software program for use with electron microprobes. Such maps are capable of providing useful information for unraveling metamorphic and tectonic histories and assisting in gathering and interpreting results using other geochronological techniques.

Desirable properties for a mineral to yield useful age information on specific petrogenetic events are listed below:

1. Highly variable composition that reflects *P-T-X* of the host rock at the time of the mineral's growth.
2. Variations in composition during mineral growth, which are preserved as distinct domains representing successive generations.
3. Slow diffusion, so zoning is stable. Also a very high "blocking temperature" so the mineral can hold chemical and isotopic signatures during metamorphism or even melting without significant diffusion.
4. Stability in a wide variety of igneous and metamorphic rocks. If a mineral is also resistant to weathering, it may be a useful constituent in clastic sediments.

Some minerals with these properties include zircon, monazite, xenotime, allanite, titanite/sphene, rutile, apatite, baddeleyite (all for U-Th-Pb dating), garnet (Sm/Nd, Lu/Hf), mica, and K-feldspar (Rb/Sr, K/Ar, $^{40}Ar/^{39}Ar$).

With the exception of the K-Ar system, geochronometry involves parent elements present in trace quantities (Rb, Sm, U, Th, etc.), which typically concentrate in accessory phases. Because accessory minerals are not necessarily controlled by major elements that reflect the *P-T* history of a rock, it may not be obvious when they crystallized. The ability to analyze a specific area of a mineral in thin section, either extracted by microdrill or in situ, is of greatest advantage when the development of that accessory mineral (or a zone within it) can be directly linked to an inherited, orogenic, or metamorphic event. Methods for doing so include:

1. Getting ages from major phases instead: K/Ar and Rb/Sr in micas, feldspars, or amphiboles; Sm/Nd and Lu/Hf in garnet.
2. Directly linking tectonic or metamorphic events to the development of datable accessory minerals using textures.
3. Linking an accessory phase to a specific reaction so that you can date a metamorphic mineral growth event (typically an isograd).
4. Chemically partitioning with a major phase to estimate development of datable mineral by its relationship to the major phase (e.g., Rubatto, 2002; Rubatto and Hermann, 2007). Partitioning can even lead to new accessory phase geothermometers (Pyle and Spear, 2000; Pyle et al., 2001).
5. Combining with geothermobarometry to add real ages (*t*) to *P-T-t* paths.

7.2 Examples of Textural Geochronology

Geochronology on minute samples of single minerals that have been linked texturally to a specific structural or metamorphic element is a rapidly proliferating field. Most examples below rely largely on the second technique listed above, which is most closely related to the subject of this chapter.

Christensen et al. (1989) used TIMS to measure $^{87}Sr/^{86}Sr$ in single garnets from southeastern Vermont (an example of technique 1 above). ^{87}Rb in K-rich matrix minerals (such as biotite) decays over time to ^{87}Sr, which was then incorporated into growing garnet (which accepts Ca, hence Sr, but not Rb). The garnets grew during the Acadian orogeny (~380 Ma). Christensen et al. (1989) managed to separately determine core and rim ages for three garnets, which allowed them to calculate the average duration of garnet growth to be 10.5 ± 4.2 Ma. Then, by measuring garnet radii, they calculated the average growth rate: 1.4 mm/Ma.

One garnet with spiral inclusions also yielded a rotational shear strain rate of $7.6 \times 10^{-7}\ a^{-1}$ (0.76 per Ma). Strain is dimensionless per time interval because it represents a ratio: the change in length of a strain ellipsoid axis divided by unit initial length. A strain rate of 0.76, simply put, means the long axis of the strain ellipsoid stretched by 76% in a million years. (More precise results require integrating the strain over shorter time intervals.) Similar isotopically based estimates of garnet growth and strain rates, as well as reaction rates, are listed by Baxter (2003). So here we see how detailed geochronology can permit estimation of the rates of some metamorphic and deformational processes.

Simpson et al. (2000) determined TIMS isotopic ratios on monazite separates from metapelites from the Everest region of Nepal. The collision of India with Asia occurred ~54 to 50 Ma, and leucogranites were emplaced 24 to 17 Ma. Previous Sr-Nd ages on garnet and U-Pb ages on bulk monazite yielded 33 to 28 and 37 to 29 Ma, respectively. Of particular importance in this study was the careful observation of textures in two rocks from which monazite was extracted. Older euhedral monazites in one sample contain oriented sillimanite inclusions parallel to S_1 in the matrix (Figure 55a), which were therefore interpreted as having grown either syn- or post-sillimanite and post S_1. Monazite separates from this rock yielded ages of 32.2 ± 0.4 Ma. Monazite in this sample is often armored within plagioclase (Figure 55b) or other minerals, which kept them from reacting in a later event and thereby preserved this early post-collision sillimanite-zone metamorphic age. Relict kyanite indicates high-pressure Barrovian-style metamorphism. Later lower-pressure metamorphism produced cordierite and irregular-shaped monazite (Figure 55c). Although there is no clear textural link, the shape and lack of armoring suggest a separate event (probably associated with the obvious low-P metamorphism), and Pb isotopes yielded 22.7 ± 0.2 Ma. The Everest granite was dated using monazite and xenotime at 21.3 to 20.5 Ma. These results place far better constraints than earlier traditional works on post-collision metamorphism, with early Barrovian style metamorphism peaking at 32 Ma and a second low-P event at 22.7 Ma (post-orogenic collapse?) and granites (probably related to collapse) emplaced at 20 to 21 Ma.

Möller et al. (2003) performed in situ SHRIMP analysis of U-Th-Pb isotopic ratios in zircons in the contact aureole around the Rogaland anorthosite/norite complex in southeastern Norway. Inherited zircons and zircon cores exhibited oscillatory zoning, which is characteristic of igneous zircon growth. They yielded an age of ~1035 Ma (the age of the initial igneous complex). A 600 to 700°C metamorphic event (M_1) followed at ~1.00 Ga, producing unzoned zircon rims with variable Th, U, and REE. A second very-high-temperature M_2 metamorphic event produced orthopyroxene, magnetite, spinel, and osumilite. Zircons occurring intergrown with, or as inclusions in, those minerals suggest syn-M_2 growth and yield SHRIMP Pb ages of 927 ± 7 Ma. Finally, zircons found outside M_2 minerals or overgrown by later garnet coronas or garnet-quartz or garnet-orthopyroxene symplectites yield ages of 908 ± 9 Ma for a retrograde

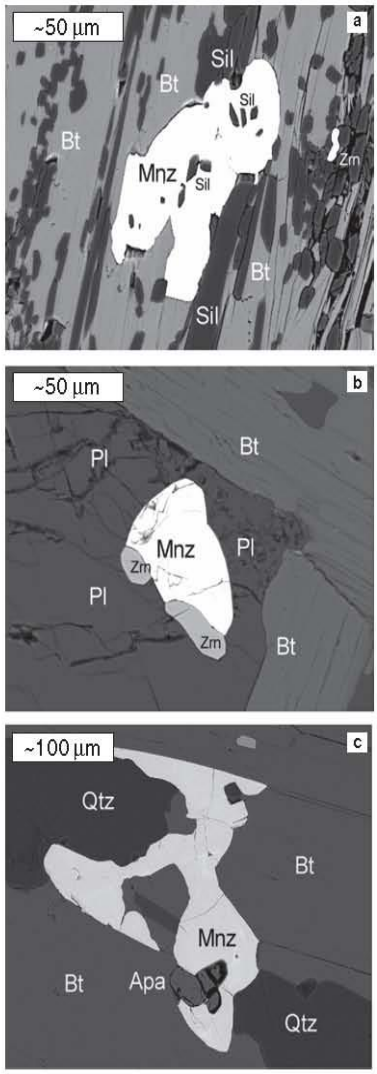

FIGURE 55 Backscattered SEM images of textural relationships of monazites from the Everest region of Nepal. (a) Well-developed M_1 monazite enveloping sillimanite inclusions aligned subparallel to external S_1 foliation. (b) Nearly euhedral M_1 monazite in the same sample surrounded by armoring plagioclase. (c) Irregularly shaped M_2 monazite in a nearby sample. From Simpson et al. (2000).

M_3 event. Earlier TIMS isotopic studies on zircon separates provided sparse evidence for the highest-grade M_2 event. Möller et al (2003) attributed this to the traditional magnetic separation of zircons, which selectively removed M_2 zircons from those analyzed because they were intimately associated with magnetite.

Cliff and Meffan-Main (2003) used the microdrill technique to extract white micas from sheared samples from the Sonnenblick Dome of the Austrian Pennine Alps. Using TIMS Rb-Sr ages, they determined a main schistosity age of 27.3 ± 0.8 Ma, which they distinguished from recrystallized micas in a later crenulation cleavage at 25.5 ± 0.3 Ma.

Whole-rock Rb-Sr dating would have sampled both mica populations and yielded an intermediate age, but careful textural and microsampling not only avoided Sr isotopic heterogeneity but took advantage of it to date individual tectonometamorphic events.

Müller et al. (2000) microsampled carbonate and quartz–chlorite from incrementally developed strain fringes of σ-type mantles (Figure 19) on pyrite porphyroclasts from a shear zone in the northern Pyrenees. The fringes developed during two distinct phases of shear (D_2 and D_3), following an earlier period of crustal shortening (D_1, which created a foliation preserved as straight inclusion trails within the pyrites). The pyrites thus grew as post-D_1 porphyroblasts but were deformed during D_2 and D_3. Figure 56 shows two examples of the porphyroclasts and fringes and the TIMS Rb/Sr dates of four fringe increments. Notice that successive increments developed between the porphyroclast and receding earlier fringe, not at the ends of the fringe tails. Figure 57 indicates the ages versus strain (ε as a percent), showing a relatively slow D_2 period (strain rate $\sim 3.5 \times 10^{-8}\ a^{-1}$) lasting from ~ 87 to 66 Ma, followed by a period of increasing D_3 strain rate ($\sim 2.4 \times 10^{-7} a^{-1}$) for about 4 Ma, correlated with an abrupt change in fiber growth direction (and interpreted as a stress field transformation from D_2 gravitational collapse to renewed D_3 crustal shortening). Compressive strain then waned to earlier D_2 rates until ~50 Ma ago.

UV-LA-ICPMS has been used to address a variety of problems. For example, Mulch et al. (2002) found that undeformed muscovite porphyroblasts in an S-C mylonite from the Italian Alps yielded a $^{40}Ar/^{39}Ar$ age of 182.0 ± 1.6 Ma (interpreted as the age of greenschist facies metamorphism, deformation and associated uplift). In situ UV-LA-ICPMS $^{40}Ar/^{39}Ar$ dating and furnace step heating (Section 9.7.2.1) within strongly deformed mica grains from the mylonite displayed a range of systematically younger apparent ages. Mulch et al. (2002) then modeled protracted cooling through argon closure temperatures with argon loss via microstructural defect-controlled intragranular diffusion pathways. From this they estimated a cooling rate of about 2°C/Ma over 50 to 60 Ma for post-182 Ma uplift of the Ivrea-Verbano Zone. Sherlock et al. (2003) dated slaty cleavage development in Welsh slates at ~396 Ma by laser step-heating and $^{40}Ar/^{39}Ar$ dating of white micas developed synkinematically in strain fringe around rigid pyritized graptolites. Accurate dating of low-grade slaty cleavage was impossible by conventional isotopic methods. Wartho and Kelley (2003) used in situ UV-LA-ICPMS and $^{40}Ar/^{39}Ar$ to date phlogopite core-rim traverses in mantle xenoliths in kimberlites. The cores yielded ages of formation of the magmatic or metasomatic events creating the parent rock, presumably in the SCLM. They then modeled the Ar loss profiles toward the rims, fit to experimentally determined Ar diffusion rates in phlogopite, to estimate the rate of ascent of the kimberlites.

Monazite U-Th-Pb dating using the electron microprobe is a rapidly proliferating technique with a wealth of applications spanning a broad range of igneous, metamorphic, sedimentary, and hydrothermal processes (see reviews by Harrison et al., 2002; and Williams et al., 2007). I shall mention only a few investigations, concentrating on ones that link ages to textures in metamorphic rocks that have experienced multiple deformation events. Monazite is a REE-phosphate mineral, which has all of the useful properties of a suitable mineral for textural geochronology listed above. Its development in metamorphic rocks is typically associated with garnet breakdown because garnet is the principal REE-bearing major silicate mineral. Monazite picks up U and Th but virtually zero Pb, so any Pb detected is derived over time from U or Th decay. We can thus use (U or Th)/Pb from *chemical* analysis (EMP) to yield an age. This enables many more labs with EM facilities but no mass spectrometer to determine ages. Because an EMP cannot distinguish isotopic ratios for direct age determination, the technique assumes that all Pb in monazite is radiogenic and that the parental U isotopes occur in average crustal proportions. If we determine total U using the microprobe, we can then estimate isotopic concentration and then Pb isotopic concentrations from each U isotope's decay rate. Both assumptions seem reasonable and justified by the good

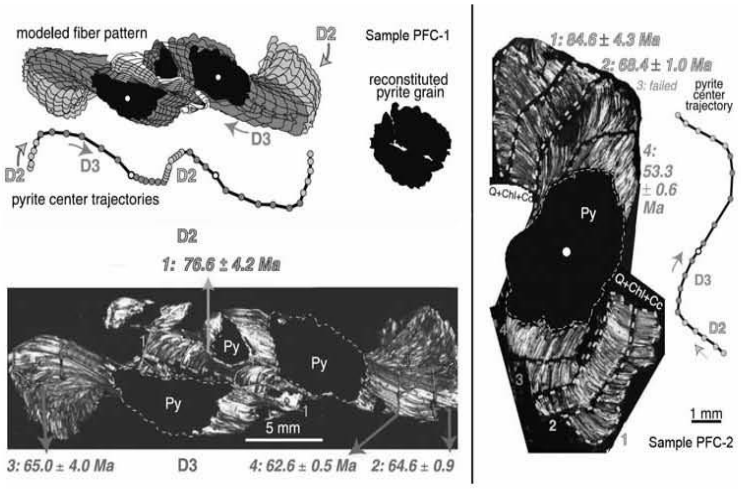

FIGURE 56 (a) Broken pyrite porphyroblast with sigmoidal fibrous carbonate–quartz–chlorite strain fringe and kinematic reconstruction above. Areas generated during D_2 and D_3 events are outlined with dashed lines in the photomicrograph (with arrows indicating the Rb-Sr ages) and shaded in the reconstruction (with arrows indicating the direction of fiber growth). (b) Photomicrograph of an unbroken pyrite porphyroblast and strain fringe with outlined growth zones and Rb-Sr ages. After Müller et al. (2000).

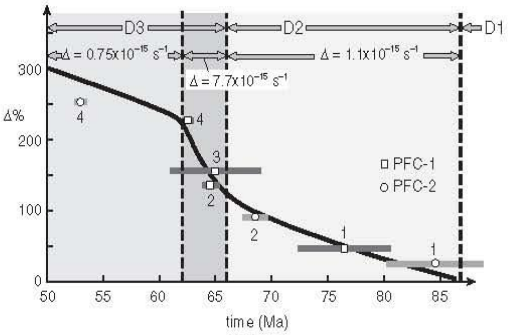

FIGURE 57 Strain in percent versus time for the two strain fringes analyzed in Figure 56. Note accelerated strain rate associated with the transition from D_2 to D_3. From Müller et al. (2000).

correlation between EMP and isotopic ages from studies addressing both. The technique is best if sufficient Pb has accumulated (i.e., early Paleozoic and older monazites). The blocking temperatures for diffusion in monazite are in excess of 800°C, so monazite can be used to date high-grade metamorphic and even many igneous events.

Pyle and Spear (2003) and Pyle et al. (2005) detected four distinct generations of monazite in migmatites sampled from the Chesham Pond Nappe of southwestern New Hampshire. The first generation occurs as high-yttrium cores in zoned monazites (bright in Figure 58). In situ EMP U-Th-Pb dating yielded an age of 410 ± 10 Ma for domain 1 cores. Pyle et al. (2005) speculated that these cores represent inherited pre-metamorphic monazites. Domain 2 monazite occurs as rims on domain 1 cores and as inclusions associated with xenotime in garnet and yield an age of 381 ± 8 Ma. Pyle and Spear (2003) attributed domain 2 development to a prograde metamorphic reaction: Chl + Qtz + Bt + Plg + Xno = Grt + Ms + Mnz + Ap + H_2O. Xenotime supplies the Y and REE necessary for monazite growth, and monazite reveals the age of this reaction and the development of garnet. Domain 3 monazite (372 ± 6 Ma) grew in the absence of xenotime and is thus is low in yttrium (dark in Figure 58). It surrounds and/or embays domain 2

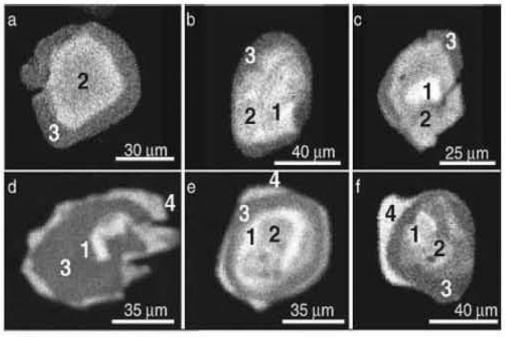

FIGURE 58 Yttrium (Y) distribution maps of zoned monazite crystals from the Chesham Pond Nappe, southwestern New Hampshire, determined by electron microprobe (EMP) analysis. Brighter areas are higher in Y. From Pyle and Spear (2003).

monazite or occurs as single grains in the matrix. It is associated with the breakdown of garnet and the development of sillimanite: Grt + Ms + Ap = Sill + Bt + Mnz. Domain 4 monazite (352 ± 14 Ma) occurs as thin discontinuous rims on earlier monazite and has very high Y content. Pyle and Spear (2003) attributed this stage to cooling and crystallization of local partial melts and leucosome development in the migmatites via the reaction: Crd + Kfs + Grt + Melt = Sil + Bt + Qtz + Plg + Mnz ± Xno. The ability to distinguish texturally separate growth stages of accessory minerals and determine ages of micron-scale domains from EMP chemical analysis is a valuable new tool. Relating those stages and domains to specific events and/or mineral reactions during prograde or retrograde metamorphism is an important step in relating these observations to the petrogenetic history of the rocks and area. Pyle and Spear (2003) used the reactions and geothermobarometry to estimate the temperatures and pressures of the dated stages of petrogenesis. They concluded that stages 2, 3, and 4 occurred along a nearly isobaric prograde path of metamorphism at about 0.3 GPa from ~500°C to melting just over 700°C. Pyle et al. (2005) related pre-metamorphic (domain 1) monazites to the local New Hampshire Granite Series of Acadian age (~390 to 410 Ma). The domains 2–4 regional metamorphism were attributed to a later heating event, ascribed to lithospheric mantle delamination and related asthenospheric upwelling. Cooling to crystallize domain 4 monazite was probably associated with overthrusting of the Chesham Pond Nappe, which may then be constrained to have begun roughly 355 Ma ago.

Mahan et al. (2006) used EMP-based geochronology to date events in high-*P*-*T* Precambrian granulites associated with the ductile Legs Lake shear zone in the Lake Athabasca region, Snowbird Tectonic Zone of the Canadian Shield. They also found multiple growth episodes (five) in zoned monazites. Figure 59 summarizes their findings. Monazite events 1 (2570 ± 11 Ma) and 2 (2544 to 2486 Ma) are high-Y and occur as inclusions in garnet. They appear to have grown during high-P-T granulite facies metamorphism prior to or coeval with garnet growth. Monazite 3 is lower in yttrium (suggesting ample garnet was present and sequestered much Y) and occurs principally in the matrix or in garnet cracks. A wide range of ages (2529 to 2160 Ma) derived from event 3 monazites suggests episodic growth with unclear significance. Event 4 monazite (1937 to 1884 Ma) was interpreted as developed during a second high-*P*-*T* granulite metamorphic event. It is also low in Y and coexists with garnet. Monazites of event 5 (~1850 Ma) were correlated with garnet breakdown (hence high-Y) to produce lower *T* and *P* retrograde biotite and cordierite (+ monazite). Mahan et al. (2006) related this uplift and hydration event to thrusting along the Legs Lake shear zone. Hydration, they speculated, was aided by loading and dehydration of the footwall metasediments with fluid channeled up the shear zone.

Finally, Dahl et al. (2005) used EMP monazite ages to constrain the timing of three Proterozoic fabric-forming events in metapelites of the Wyoming craton in South Dakota. Figure 60 shows the textures. An east-northeast-trending

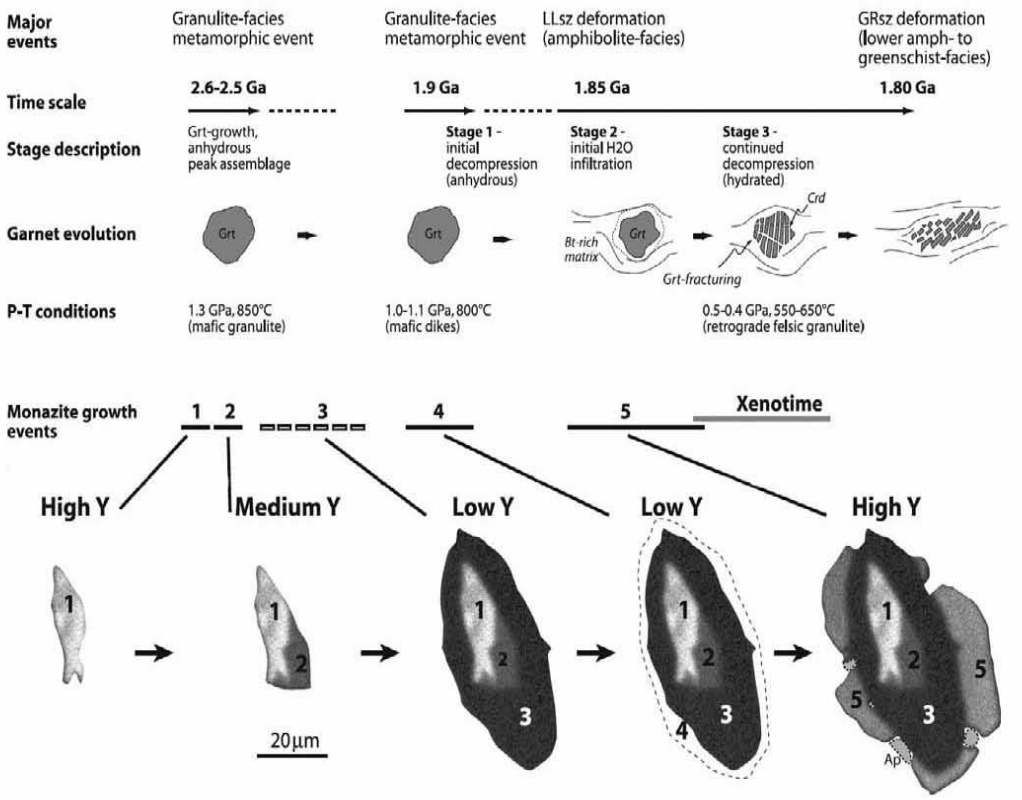

FIGURE 59 Summary model for the evolution of felsic granulites in retrograde shear zones, Snowbird Tectonic Zone, Saskatchewan, Canada. Bottom images are yttrium element maps of a zoned monazite crystal from which age determinations for the events have been derived. (Brighter areas are higher in Y.) Possible intermediate periods of resorption are not shown. LLsz = Legs Lake shear zone. After Mahan et al. (2006).

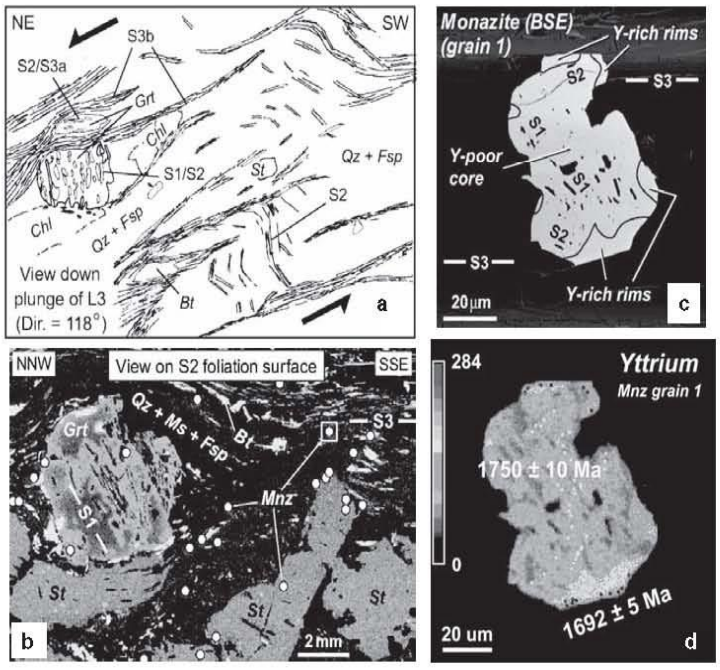

FIGURE 60 Polydeformed textures and monazite in a metapelite from the eastern Wyoming craton, Black Hills, South Dakota. (a) Sketch of textures viewed down plunge of L_3 lineation showing S_1/S_2 in garnet porphyroblasts, and S_2 in microlithons between S_3 overprint. (b) Photomicrograph parallel to S_2 surface showing S_1 in garnet and S_3 in matrix. (S_2 cannot be seen because it is in the plane of the section). The square in the upper right surrounds the monazite in c and d. (c) Backscattered SEM image of monazite with internal S_1 in core leading into spiral S_2 toward rim and later Y-rich overgrowth. (d) Yttrium element map of the same monazite crystal (brighter areas are higher in Y) showing spots analyzed for ages. After Dahl et al. (2005).

S_1 is attributed to a north-verging nappe/thrusting accretion event and is preserved only in garnet and staurolite porphyroblasts. S_2 (attributed to folding associated with ~east-west collision of continental fragments) is a rotational extension of S_1 in some porphyroblasts and dominates many microlithons between the dominant foliation, S_3, which overprinted and transposed S_2 and has been ascribed to doming associated with intrusion of a local granite. The consistent east-northeast orientation of S_1 in several porphyroblasts suggests they didn't rotate during growth (in spite of the spiral S_2 tails). EMP ages from a complex monazite (in the small square in Figure 60b and magnified in the BSE image Figure 60c), and a Y element map (Figure 60d) yielded ages of 1750 ± 10 Ma for the core with internal S_1 and S_2 (providing a minimum age for the foliation events) and 1692 ± 5 Ma for the high-Y rim, which truncates S_1/S_2 and is associated with resorption textures of garnet (supplying Y to monazite). This later event is best correlated with intrusion of the nearby Harney Creek granite.

Hopefully, this section has given you an idea of the many applications of analyzing individual minerals, or even mineral zones, to determine the ages of specific metamorphic, tectonic, or igneous events to which the minerals can be correlated. I'm sure many more creative uses will be developed and techniques refined.

Summary

Metamorphic textures develop in the solid state as mineral grains interact with their neighbors during deformation, recrystallization, and/or growth. Applied stress commonly accompanies metamorphism, whereby it causes deformation (strain) in solids. Crystalline deformation at low temperatures is dominated by cataclastic flow, involving mechanical breaking or crushing of crystals. Plastic deformation takes over at higher grades where no cohesion is lost. Defect and dislocation migration greatly facilitate plastic deformation. Recovery involves migration of defects to grain boundaries or new subgrain boundaries, leaving behind regions of reduced lattice strain. Static recrystallization involves a more advanced migration of grain or subgrain boundaries to produce a mosaic of low-strain grains. Deformation and recovery/recrystallization generally interact because deformation adds energy to crystal lattices. Higher energy states are less stable, so processes that reduce it, such as recrystallization, are encouraged. A strained crystal is therefore more apt to recrystallize than a neighboring unstrained one. Dynamic recrystallization is the simultaneous action of deformation and recovery/recrystallization. It typically produces a good crystallization schistosity. If recrystallization lasts longer than deformation or occurs in a static environment, such as a contact aureole, it is called annealing.

The hallmark texture of contact metamorphism in a low-pressure relatively static environment is granoblastic polygonal. It develops best in monomineralic quartz or feldspar regions and is characterized by polygonal grains with straight boundaries, typically meeting at three-grain boundaries in thin section at 120° angles. Minerals that tend more toward euhedral or subhedral shapes develop decussate texture. Porphyroblasts of larger metamorphic minerals in a finer groundmass are common in (although certainly not restricted to) contact metamorphism, as are inclusion-bearing poikiloblasts.

Cataclastic processes dominate over recovery and recrystallization in fault/shear zones, particularly at shallow depths, where broken, crushed, and bent pre-deformational grains (called *clasts*) are common. Shear zones typically broaden with depth, where shear is distributed while recovery processes join cataclasis as dynamic recrystallization. Mylonitic foliations are generally produced. Determining the sense of shear in zones no longer active can be challenging, and a number of shear-sense indicators have been proposed.

Textures of regional (orogenic) metamorphism can be very complex (and thus very informative). Orogeny may involve several cycles and events of deformation and metamorphism, each leaving textural and mineralogical traces. Deciphering multiple foliations, lineations, and periods of mineral growth requires careful microscopic observation and practice. The pattern of inclusions within poikiloblasts (S_i), when developed, may be particularly informative, as they may record events obliterated in the matrix by later deformation.

Replacement and reaction textures typically develop when reactions fail to run to completion. Such textures capture metamorphic reactions texturally and indicate the nature, direction, and progress of a reaction. We can use these textures to understand the nature of the protolith and the changing conditions experienced by a sample.

Technological advances are now allowing us to extract age information from very small volumes of a mineral, even from grains observed in thin section. This is opening up some exciting avenues of research in which the timing of individual tectonic/metamorphic, igneous, or sedimentary events may be determined. To be meaningful, these ages must be related to other critical petrologic information, such as textures, mineral reactions, and/or thermodynamic models that estimate pressures and temperatures of evolving rocks.

TABLE 1 Textures of Metamorphic Rocks

General Textural Terms:	
Relict	A remnant texture inherited from the parent rock and not yet overprinted or obscured by metamorphism.
Blasto-	A prefix indicating a relict texture (e.g., "blastophitic").
-blast	A suffix indicating a texture of true metamorphic origin.
Idioblastic	Euhedral
Hypidioblastic (subidioblastic)	Subhedral
Xenoblastic	Anhedral
Porphyroblast	A larger metamorphic mineral in a matrix of smaller ones.
Poikiloblast	A porphyroblast with numerous inclusions.
Skeletal, web	An extreme variation of a poikiloblast in which the including mineral occurs as a thin, optically continuous film surrounding the inclusions.
Nodular	Ovoid porphyroblasts.
Spotted	Used to describe the appearance of small (commonly ovoid) porphyroblasts in hand specimen.
Depletion haloes	Zones surrounding porphyroblasts that have had one or more minerals removed by reaction and diffusion to the growing porphyroblast.
Non-Foliated Texture:	
Granoblastic Polygonal (polygonal mosaic)	Equidimensional generally anhedral crystals of approximately equal size with regular polygonal shapes (usually 5- or 6-sided) and fairly straight boundaries meeting at triple junctions. Best displayed in monomineralic rocks (marble, quartzite). Poymineralic rocks approach this, but are modified by the differences in degree of idioblastic form.
Decussate	Randomly oriented interlocking subhedral prisms. Tends to form in minerals with strong anisotropy of surface energy, such as mica, pyroxene, or hornblende.
Symplectite	An intimate intergrowth of two or more minerals that grew simultaneously.
Corona	A rim of one or more minerals surrounding another mineral.
Moat	A coronitic rim that completely surrounds a mineral.
Textures of Dynamic Metamorphism:	
Cataclastic	A general texture resulting from the predominantly brittle deformation of minerals (it typically involves grain-size reduction).
Mylonitic	Foliated cataclastic/plastic texture.
Pseudotachylite	A dynamically metamorphosed rock containing glass generated by localized shear melting.
Undulose extinction	Irregular extinction resulting from deformation of the lattice of a crystal.
Cracked	Crystals showing obvious cracks.
Crushed	Crystals are ground by shear and exhibit fine-grained margins derived from the original larger crystals. The proportion of crush material can vary considerably and even comprise 90% of the rock.
Deformation band	Dimensionally elongated bands within a crystal resulting from cracking or slip.
Porphyroclast	A large, relict crystal in a fine crush matrix.
Mortar	Rounded porphyroclasts rimmed by a crush matrix.
Ribbon	Very elongate crystals (usually quartz) resulting from cataclasis and intense plastic deformation.
Shredded	The intense breakup of minerals (usually phyllosilicates) along cleavages to produce very fine locally crushed margins.
Kink band	Zones bounded by parallel planes in which some feature, usually cleavages, have a different orientation.
Deformation twin	Twinning or lamellae produced by deformation. Common in carbonates and recognized in feldspars when the twins/lamellae are bent or dominantly wedge shaped.
Textures of Dynamic Metamorphism:	
Polygonized	Incipient recrystallization where larger deformed crystals break down into smaller, undeformed subgrains. The outlines of the larger crystals are still distinguishable.
Sutured	Incipient recrystallization in which the larger crystals differentially incorporate the marginal crush matrix to produce an interdigitation of grain boundaries.

(*Continued*)

TABLE 1 Textures of Metamorphic Rocks (*Continued*)

Textures of Dynamic Metamorphism:

Oblique foliation	Foliations that cut across the foliation developed due to shear offsets.
Shear band cleavage or S-C texture	A texture that has shear bands (or C foliations), which are spaced cleavages that transect well-developed mineral foliation (S foliation) at a small angle.
Mantled porphyroclast	Resistant porphyroclast with a rim that has the same mineralogy as the porphyroclast. The mantles are assumed to be derived from the porphyroclast by grinding.
Augen, flaser	Eye-shaped mantled porphyroclasts.
Quarter structure	A structure in which the four quadrants defined by the foliation and its normal are not symmetric.
Quarter fold	Small fold in the foliation around porphyroclasts due to drag.
Quarter mat	Concentration of mica resulting from dissolution of quartz in the shortened quadrants of porphyroclast.

Texture of Regional Metamorphism:

Foliation	Any planar fabric element.
Lineation	Any linear fabric element.
Spaced foliation	A foliation developed in zones separated by non-foliated "microlithons."
Continuous foliation	A foliation that is not spaced, but occurs continuously.
Cleavage	Any type of foliation in which the aligned platy phyllosilicates are too fine to see with the unaided eye.
Slaty cleavage	Fine-grained continuous cleavage.
Crenulation cleavage	A cleavage or schistosity that becomes microfolded.
Schistosity	A planar orientation of elongated mineral grains or grain aggregates produced by metamorphic processes. Aligned minerals are coarse enough to see with the unaided eye.
Gneissose structure	Either layered by metamorphic processes or a poorly developed schistosity.
Layering, banding	A foliation consisting of alternating layers of different composition.
Prekinematic	Refers to crystals which were present prior to deformation/metamorphism and were deformed.
Synkinematic	Refers to crystals which grew during deformation/metamorphism.
Postkinematic	Refers to crystals which grew after deformation.
Inter-kinematic	Mineral growth that is post-kinematic to one event and pre-kinematic to another.
S-surface	A foliation or planar fabric in a deformed rock. Commonly numbered (S_1, S_2, S_3, etc.) if there are successively developed foliations. S_0 is reserved for pre-metamorphic foliations, such as bedding, flow banding, cumulate layering, etc.
S_i	Internal *S*, the alignment of inclusions within a poikiloblast.
S_e	External *S*, the foliation of the matrix outside a poikiloblast.
L	A lineation (can also have L_1, L_2, etc.).
Pressure shadow	Concentration of a matrix mineral in low-stress areas adjacent to a porphyroblast due to pressure solution (solution transfer) and re-precipitation.
Wrapped	A foliation compressed about a pre-kinematic porphyroblast (or possibly bowed out by the growing porphyroblast).
Helicitic	Folded internal *S*, indicates a post-kinematic porphyroblast.
Spiral (rotational, snowball)	Showing a texture, such as a spiraled inclusion trail, that indicates rotation.
Polygonal arc	A post-kinematic recrystallization of bent crystals into an arcuate pattern of smaller straight crystals. A form of polygonization.

See also the glossary in Vernon, 2004.

Key Terms

See Table 1 for definitions of many textural terms.
Texture (micro-structure)/fabric, structure
Penetrative features
-blast, blasto-
Cataclastic flow
Solution transfer
Point/line defects
Slip system
Dislocation glide
Strain hardening
Dislocation creep
Undulose extinction
Deformation twinning
Recovery
Grains/subgrains
Recrystallization

Grain boundary migration/bulging/subgrain rotation
Solid-state diffusion creep
Crystalplastic deformation
Grain boundary sliding
Serrated/sutured grains
Dynamic recrystallization
Annealing/static recrystallization
Granoblastic polygonal/polygonal mosaic
Decussate
Porphyroblast, poikiloblast
Skeletal/spongy/web
Depletion halo
Nodular, spotted
Crystalloblastic series
Crystal size distribution (CSD)
Clasts, porphyroclasts, mortar, ribbons
Pseudotachylite
Polygonization, coalescence
Shear-sense indicators: oblique foliations, C-type and C′-type shear bands, S-C mylonites, mantles porphyroclasts, complex objects, mica-fish, quarter folds/mats, asymmetric folds
Tectonic event, deformational phase
Metamorphic cycle, event, phase
Tectonite
Foliation (primary, continuous, spaced, cleavage, schistosity, crenulation cleavage)
Microlithons, cleavage domains
Lineations (stretching, elongate elements, fold axes, intersecting planes)
Mechanisms (mechanical rotation, oriented growth, crystal-plastic deformation, transposition, pressure solution)
Mimetic growth
Gneissose structure, metamorphic differentiation
Kink bands
Boudinage/boudin
Petrofabric diagram
S-tectonite: S_0, S_1, S_2, S_3, . . .
L-tectonite: L_0, L_1, L_2, L_3, . . .
D_1, D_2, M_1, M_2 events
Pre-kinematic, syn-kinematic, and post-kinematic mineral growth
S_i, S_e
Armored relic
Helicitic folds, polygonal arcs
Spiral, snowball
Reaction rim, corona, moat
TIMS, LA-ICPMS, IMP, EMP

Review Questions and Problems

Review Questions and Problems are located on the author's web page at the following address: **http://www.prenhall.com/winter**

Important "First Principle" Concepts

- Deformation adds strain energy to the lattices of crystals in the form of bond bending and defects. Systems tend naturally toward states of lowest energy, so strained lattices are less stable than unstrained ones. Recovery and recrystallization are ways to reduce that stored energy, so are assisted by deformation.
- Orogenic structures and textures are "fractal" in the sense that deformational features, orientations, and styles are typically evident and correlative from the scale of the mountain to the outcrop to the hand specimen and thin section.
- Orogenic deformation and metamorphism may involve several events that are neither synchronous nor universal across the orogen. Careful petrographic work, combined with structural analysis and good field work, is required to unravel such complex histories.

Suggested Further Readings

Barker, A. J. (1990). *Introduction to Metamorphic Textures and Microstructures*. Blackie. Glasgow.

Jamieson, R. A. (1988). Textures, sequences of events, and assemblages in metamorphic rocks. In: *Short Course on Heat, Metamorphism, and Tectonics* (eds. E. G. Nisbet and C. M. R. Fowler). Short Course **14**, 213–257. Mineralogical Association of Canada.

Müller, W. (2003). Strengthening the link between geochronology, textures, and petrology. *Earth Planet. Sci. Lett.*, **206**, 237–251.

Parrish, R. R. (1990). U-Pb dating of monazite and its application to geological problems. *Can. J. Earth Sci.*, **27**, 1431–1450.

Passchier, C. W., and R. A. J. Trouw. (2005). *Mictotectonics*. Springer-Verlag. Berlin.

Platt, L. (1976). A Penrose Conference on cleavage in rocks. *Geotimes*, **21**, 19–20.

Spry, A. (1969). *Metamorphic Textures*. Pergamon. Oxford, UK.

Vance, D., W. Müller, and I. M. Villa (eds.). (2003). *Geochronology: Linking the Isotopic Record with Petrology and Textures*. Special Publication **220**. The Geological Society. London.

Vernon, R. H. (2004). *A Practical Guide to Rock Microstructure*. Cambridge University Press. Cambridge, UK.

Williams, M. L., M. J. Jercinovic, and C. J. Hetherington. (2007). Microprobe monazite geochronology: Understanding geologic processes by integrating composition and chronology. *Ann. Rev. Earth Planet. Sci.*, **35**, 137–175.

Yardley, B. W. D., W. S. McKenzie, and C. Guilford. (1990). *Atlas of Metamorphic Rocks and Their Textures*. Longman. Essex, UK.